การวิจัยและพัฒนาพอลิโพรพิลีนคอมโพสิตนำไฟฟ้าเพื่อใช้เป็นบรรจุภัณฑ์สำหรับ
อุปกรณ์อิเล็คทรอนิกส์

นายสาโรช พรหมดี

RESEARCH AND DEVELOPMENT OF CONDUCTIVE POLYPROPYLENE COMPOSITE FOR
ELECTRONIC PACKAGING

Mr. Sarote Phromdee

A Thesis Submitted in Partial Fulfillment of the Requirements

for the Degree of Master of Engineering Program in Chemical Engineering

Department of Chemical Engineering

Faculty of Engineering

Chulalongkorn University

Academic Year 2013

Thesis Title	RESEARCH AND DEVELOPMENT OF CONDUCTIVE POLYPROPYLENE COMPOSITE FOR ELECTRONIC PACKAGING
By	Mr. Sarote Phromdee
Field of Study	Chemical Engineering
Thesis Advisor	Associate Professor Sarawut Rimdusit, Ph.D.
Thesis Co-Advisor	Sunan Tiptipakorn, D.Eng.

Accepted by the Faculty of Engineering, Chulalongkorn University in Partial Fulfillment of the Requirements for the Master's Degree

⋯⋯⋯⋯⋯⋯⋯⋯⋯⋯⋯⋯⋯⋯⋯Dean of the Faculty of Engineering

(Professor Bundhit Eua-arporn, Ph.D.)

THESIS COMMITTEE

⋯⋯⋯⋯⋯⋯⋯⋯⋯⋯⋯⋯⋯⋯⋯Chairman

(Associate Professor Muenduen Phisalaphong, Ph.D.)

⋯⋯⋯⋯⋯⋯⋯⋯⋯⋯⋯⋯⋯⋯⋯Thesis Advisor

(Associate Professor Sarawut Rimdusit, Ph.D.)

⋯⋯⋯⋯⋯⋯⋯⋯⋯⋯⋯⋯⋯⋯⋯Thesis Co-Advisor

(Sunan Tiptipakorn, D.Eng.)

⋯⋯⋯⋯⋯⋯⋯⋯⋯⋯⋯⋯⋯⋯⋯Examiner

(Pimporn Ponpesh, Ph.D.)

⋯⋯⋯⋯⋯⋯⋯⋯⋯⋯⋯⋯⋯⋯⋯External Examiner

(Parkpoom Lorjai, Ph.D.)

สาโรช พรหมดี : การวิจัยและพัฒนาพอลิโพรพิลีนคอมโพสิตนำไฟฟ้าเพื่อใช้เป็นบรรจุ
ภัณฑ์สำหรับอุปกรณ์อิเล็คทรอนิกส์. (RESEARCH AND DEVELOPMENT OF
CONDUCTIVE POLYPROPYLENE COMPOSITE FOR ELECTRONIC PACKAGING)
อ.ที่ปรึกษาวิทยานิพนธ์หลัก: รศ. ดร. ศราวุธ ริมดุสิต, อ.ที่ปรึกษาวิทยานิพนธ์ร่วม: ดร.
สุนันท์ ทิพย์ทิพากร, 86 หน้า.

โดยทั่วไปบรรจุภัณฑ์ที่สามารถนำไฟฟ้าได้จะต้องมีค่าความต้านทานไฟฟ้าเชิงปริมาตร
ต่ำกว่า 10^4 โอห์ม·เซนติเมตร การทำให้บรรจุภัณฑ์พอลิโพรพิลีนมีสภาพการนำไฟฟ้าอยู่ในช่วง
ดังกล่าวสามารถทำได้โดยการใช้คาร์บอนแบล็คที่เป็นสารตัวเติมนำไฟฟ้า สำหรับการทำให้
กระบวนการผลิตพอลิโพรพิลีนนำไฟฟ้ามีต้นทุนต่ำนั้นมีวิธีที่ได้รับความนิยมคือการลดปริมาณการ
เติมคาร์บอนแบล็คในคอมโพสิตนำไฟฟ้าให้น้อยที่สุด ด้วยการนำพอลิเมอร์อีกชนิดหนึ่งมาผสมเข้า
กับพอลิโพรพิลีน โดยมีลักษณะการผสมที่ไม่ผสมเข้ากัน หรือผสมเข้ากันได้บางส่วน และให้
คาร์บอนแบล็คกระจายตัวอยู่ในส่วนวัฏภาคใดวัฏภาคหนึ่งของพอลิเมอร์ที่ไม่เข้ากัน ซึ่งจะทำให้
เกิดปรากฏการณ์ดับเบิลเพอร์โคเลชัน (Double percolation) ที่ช่วยลดปริมาณการเติมคาร์บอน
แบล็คให้น้อยลงมากที่สุด ในงานวิจัยนี้บรรจุภัณฑ์คอมโพสิตนำไฟฟ้าได้เตรียมขึ้นจากการผสมพอ
ลิเมอร์ระหว่างพอลิโพรพิลีนกับยางเอทิลีนโพรพิลีน ที่อัตราส่วน 100/0 ถึง 50/50โดยน้ำหนัก ใช้
คาร์บอนแบล็คเป็นสารตัวเติมนำไฟฟ้าในปริมาณ 0-30 เปอร์เซ็นต์โดยน้ำหนัก โดยผสมกันใน
เครื่องผสมที่อุณหภูมิ 200 องศาเซลเซียส เป็นเวลา 10 นาที จากนั้นอัดขึ้นรูปที่อุณหภูมิเดียวกัน
จากการศึกษาพบว่าพอลิเมอร์ผสมระหว่างพอลิโพรพิลีนกับยางเอทิลีนโพรพิลีนมีพฤติกรรมเป็น
พอลิเมอร์ผสมที่สามารถผสมเข้ากันได้บางส่วน และสามารถเพิ่มเปอร์เซ็นต์การยืดดึงของพอลิ-
โพรพิลีนและพอลิโพรพิลีนคอมโพสิตขึ้นที่เติมคาร์บอนแบล็คได้อย่างมาก ยิ่งไปกว่านั้นยังเห็นได้
ชัดว่าพอลิเมอร์ผสมยังช่วยทำให้ช่วง เพอร์โคเลชันเทรชโฮลด์ (Percolation threshold) มีค่า
ต่ำลง และเพิ่มค่าการนำไฟฟ้าได้ดีกว่าการใช้พอลิโพรพิลีนเพียงชนิดเดียว เมื่อพิจารณาค่าความ
ต้านทานไฟฟ้าของคอมโพสิตที่เกิดจากพอลิเมอร์ผสม พบว่า สามารถลดปริมาณการเติมคาร์บอน
แบล็คให้ลดลงได้ถึง 50 เปอร์เซ็นต์ เมื่อเทียบกับการใช้พอลิโพรพิลีนชนิดเดียว ผลการตรวจสอบ
การกระจายตัวของอนุภาคนำไฟฟ้าด้วยกล้องจุลทรรศน์อิเล็กตรอนแบบส่องกราด พบว่า อนุภาค
นำไฟฟ้ามีการกระจายตัวบริเวณของยางเอทิลีนโพรพิลีนดีกว่าในพอลิโพรพิลีน นอกจากนั้นสมบัติ
การรับแรงดึงและการทนแรงกระแทกของคอมโพสิตนำไฟฟ้าพบว่าผ่านเกณฑ์ตามที่อุตสาหกรรม
ต้องการ อีกทั้งต้นทุนวัตถุดิบที่สามารแข่งขันได้พอลิเมอร์คอมโพสิตนำไฟฟ้า จึงมีความเป็นไปได้
เป็นอย่างมากที่จะใช้เป็นบรรจุภัณฑ์สำหรับอุปกรณ์อิเลคทรอนิกส์ได้

ภาควิชา	วิศวกรรมเคมี	ลายมือชื่อนิสิต	....
สาขาวิชา	วิศวกรรมเคมี	ลายมือชื่อ อ.ที่ปรึกษาวิทยานิพนธ์หลัก	....
ปีการศึกษา	2556	ลายมือชื่อ อ.ที่ปรึกษาวิทยานิพนธ์ร่วม	....

5570414521 : MAJOR CHEMICAL ENGINEERING
KEYWORDS: CONDUCTIVE POLYMER COMPOSITE / CARBON BLACK / PERCOLATION THRESHOLD / ELECTRICAL PROPERTIES

SAROTE PHROMDEE: RESEARCH AND DEVELOPMENT OF CONDUCTIVE POLYPROPYLENE COMPOSITE FOR ELECTRONIC PACKAGING. ADVISOR: ASSOC. PROF. SARAWUT RIMDUSIT, Ph.D., CO-ADVISOR: SUNAN TIPTIPAKORN, D.Eng., 86 pp.

Volume resistivity of less than 10^4 Ω.cm is required for typical electrically conductive packages. Conductive polypropylene (PP) packages with the above level of conductivity value can be achieved by a use of carbon black (CB) as conductive filler. To maintain processability of PP with low cost, minimal amount of CB is preferable in the formulated conductive composites. By introducing a second polymer with immiscible or partially miscible nature to the first polymer, and if the conductive filler is localized in one polymer phase, a system of double percolation with minimal filler content can be achieved. In this work, electrically conductive composite packages are prepared from polymer blends of PP and ethylene propylene rubber (EPR) with CB as conductive filler (PP/EPR/CB). PP/EPR mixtures at the weight ratios between 100/0 to 50/50 were blended with CB filler with loadings ranging from 0 to 30 wt% by melt mixing in an internal mixer at 200 $^{\circ}$C for 10 min, followed by compression molding at the same temperature. The PP/EPR blends were found to be partially miscible in nature with significant enhancement in percent elongation of the PP and its CB-filled composites. The blends evidently provided a reduced percolation threshold by one half with the obtained electrical conductivity values greater than those of the CB filled PP composites. Scanning electron microscopy has been used to verify the preferential location of the conductive CB particles in EPR domains better than in the PP domains and to reveal the partially miscible blend morphology developed. The obtained tensile and impact properties of conductive composites were also found to provide the values meet those industrial requirements with a competitive material cost. The obtained conductive composites show great possibility of specially designed polymer compositions for electronic package applications.

Department:	Chemical Engineering	Student's Signature	....
Field of Study:	Chemical Engineering	Advisor's Signature	....
Academic Year:	2013	Co-Advisor's Signature	....

ACKNOWLEDGEMENTS

CONTENTS

LIST OF TABLES

Page

LIST OF FIGURES

CHAPTER I

INTRODUCTION

1.1 Overview

Static charge is a serious problem for electronics, dangerous materials, fine powders and fuels if their packaging materials are not statically dissipative [1]. The expected annual losses in products containing sensitive electronics due to electrostatic discharge (ESD) during manufacturing, assembly, storage and shipping are in billions of dollars [2]. Consequently, an ESD control system associated to production and handling systems is necessary. Advantages of using plastics in packaging applications lead to an effort in developing conductive/static dissipative plastic materials. Packaging materials are classified into conductive, static dissipative and insulative according to their volume/ surface resistivity. According to the electronic industry association (EIA) and the electrostatic discharge association (ESDA) standards, static dissipative material volume resistivity is in the range of 10^4–10^{11} Ω cm [3]. Materials with resistivities higher or lower than this range are considered insulator or conductor, respectively.

Incorporating conductive filler is the best-known method of making polymer electrically conductive. Addition of carbon black (CB) powder into plastics is satisfactory because CB tends to form network structure by which desired conductivity in a range of 10^1 to 10^6 Ω/square and 10^1 to 10^4 Ω.cm [1, 4]. For many simple binary systems the percolation threshold is 12–15 vol% filler [5], although it can be greatly lower or higher [6] depending on the conductivity level required. Lowering this percolation threshold performs to be an effective way of reducing the required amount of conductive filler and hence the processing-related problems, while keeping the all-important conductivity at sufficient levels and minimizing issues arising from mechanical properties. Nevertheless, for binary systems (i.e. carbon black mixed with one polymer) there is a direct and intrinsic coupling between the

electrical percolation, which gives a low conductivity, and the mechanical percolation, which decreases processing ability. Alternatively, binary immiscible or partially miscible blends can be designed in a technique that favors the dispersion of CB particles in the minor component of co-continuous blends [7].

Several studies [6-13] have shown that the selective localization of conducting particles in one of the phases or at best at the interface of co-continuous two-phase polymer blend is a very effective strategy to decrease the CB percolation threshold. Such systems in which conductive fillers form connective network within one phase or at interface of co-continuous blends can be defined as double percolation or percolation in percolation. According to percolation theory, double percolation or connectivity of filler within the connective phase gives rise to the reduced critical concentration or percolation threshold of the filler [8]. Consequently, reducing CB loading in conductive polymer composites is a major research challenge.

The purpose of this research is to minimize the use of CB in conductive composite and their contents on electrical, mechanical and thermal properties of the resulting conductive polypropylene composite for electronic packaging applications will be examined. The obtained polypropylene composite will also be compared with commercial conductive polypropylene.

1.2 Objectives

1. To minimize the use of CB in conductive polymer blends by controlling phase morphology.
2. To investigate systematically the effect of conductive filler content on electrical, mechanical and thermal properties of conductive PP/EPR composites for an electronic packaging application.

1.3 Scope of the study

1. Prepare PP/EPR blends by using PP (1102H, IRPC) and EPR (3325M, IRPC) with MFI of 2 and 9 g/10 min (2.16 kg/230°C), respectively via internal mixer.

2. Determine the optimum content of EPR in PP/EPR blends by varying EPR content from 0 to 50 wt%.

3. Prepare conductive PP/EPR composite by using carbon black as conductive filler ranging from 0-30 wt%.

Properties of carbon black (ENSACO 250 G) used.

Property Test Method	Unit	ENSACO 250 G
BET Nitrogen Surface Area ASTM D3037	m^2/g	65
DBP Absorption ASTM D2414	ml/100 g	190
Pour Density ASTM D1513	kg/m^3	170
Ash Content ASTM D1506	%	0.01
pH ASTM D1512		8-11

4. Fabricate conductive PP/EPR composites by using compression molder.

5. Investigate the properties of conductive PP/EPR composites as followed:

Physical properties

- Specific gravity

- Viscosity (Rheometer)

- Melt flow rate (230°C/2.16 kg)

- Morphology (SEM)

- Electrical properties

- Resistivity (Electrometer)

- Mechanical properties

- Tensile properties (UTM)

- Impact properties (Impact tester)

- Storage and loss modulus (DMA)
- Thermal properties
- Glass transition temperature (DSC or DMA))
- Degradation temperature and char yield (TGA)

1.4 Procedure of the Study

1. Prepare chemicals, apparatus and equipment for this research such as PP, EPR and CB.

2. Determine mixing or processing conditions of the PP, EPR and their blends.

3. Examine PP/EPR blends by varying compositions of EPR from 0 to 50 wt% and evaluate physical and mechanical properties.

4. Examine conductive PP/EPR/CB composite by using minimization of CB.

5. Evaluate electrical, mechanical and thermal properties of conductive PP/EPR/CB composites.

6. Summarize the optimum ratios of PP/EPR/CB composite in terms of physical, mechanical and thermal properties, which are recommended for commercial products.

CHAPTER II

THEORY

2.1 Morphology of Polymer Blends

The morphology produced during mixing depends on the interfacial tension between the phases, the blend ratio, the viscosities and relative viscosities, elasticities, and processing condition. Blending of two polymers generally results in the formation of an immiscible heterogeneous two-phase system according to thermodynamic principles. Commonly, the morphology of multiphase polymer blends depends on the composition, the rheological properties of the individual components, and blending condition [14]. Several morphologies can be obtained over the whole composition range. At low concentrations, the morphology of dispersed phase-matrix is found in which the shape of the dispersed phase can be spherical, fibrillar, or lamella depending on the shear history during processing. As the blend ratio increases, a dispersed phase begins to evolve into irregular shapes, though still recognizable as separate domains, due to coalescence. Additional increase in the amount of the dispersed phase will lead to phase inversion, before which a co-continuous structure is formed. That is both phase seem to be continuous throughout the observed field. Yet higher phase ratios yield an inversion where the dispersed phase becomes the continuous matrix and the matrix phase becomes separated domains.

An example of morphological evolution is shown in the binary images in Figure 2.1, taken from the work of Skochdopole et al. [15].
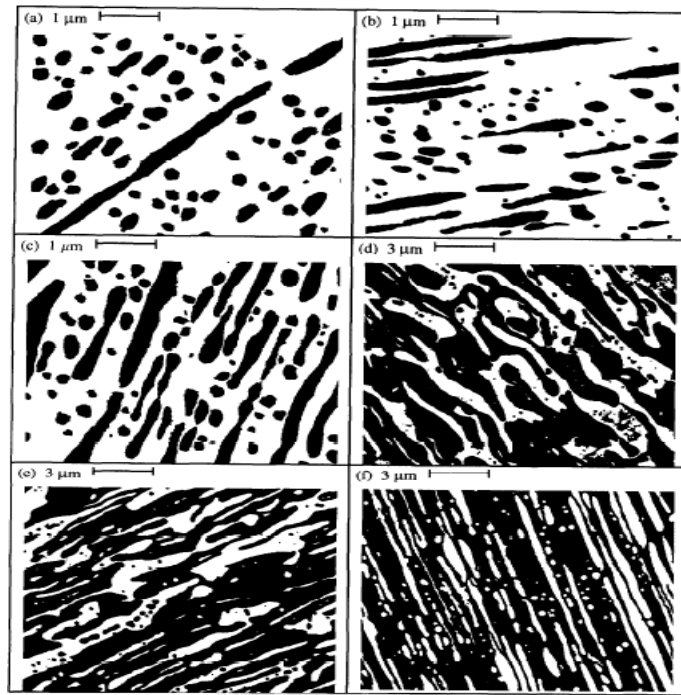
Figure 2. 1: Binary images of PC/SAN blends with varying composition. The light phase is PC and dark phase is: (a) 10%, (b) 20%, (c) 30%, (d) 40%, (e) 50% and (f) 75% SAN [16].

The dark phase is a 70/30 styrene/acrylonitrile copolymer (SAN) and the light phase is polycarbonate (PC). The morphologies in Figure 2.1 (a) to (c) shows discrete domains of SAN in a matrix of PC with domain shape becoming less regular with increasing fraction of SAN. Figures 2.1 (d) and (e) exhibit co-continuity of SAN and PC, although Figure 2.1 (e) shows that the blend is just beginning to show formation of discrete domains of PC in SAN. In Figure 2.1 (f), the morphology has reversed, with domains of PC dispersed in a matrix of SAN.

Generally, the morphologies of polymer blends are straight related to the viscoelastic properties of their individual components. The point of phase inversion at which co-continuity is observed may be related to the rheological appearances of the pure materials through a semi-empirical model [14].

Avgerpoulos et al. [17] used a relationship between the torque ratio and the composition (volume fraction) expressed as:

$$\frac{\tau_1}{\tau_2} = \frac{\phi_1}{\phi_2} \qquad (2.1)$$

where τ_i is the torque during mixing in an internal mixer and ϕ_i is the volume fraction of polymer i.

At the moment, the underlying mechanism of nanoparticle-induced co-continuity is unclear. According to Paul and Barlow [18], the condition for phase inversion from a dispersed structure to a co-continuous one is expressed as:

$$\frac{\phi_1}{\phi_2} = \frac{\eta_1}{\eta_2} \qquad (2.2)$$

where ϕ_i is the volume fraction, η_i is melt viscosity, and i denotes phase 1 or 2

That is an increase in the volume fraction or a decrease in the viscosity of the minor polymer would improve its continuity in the matrix. The nanoparticle's selective location will actually give additional volume to the minor polymer. Nevertheless, in the case of the CB-filled PS/PE system, the CB content is too low (about 4 wt%) to reduce the phase inversion point of PE from 40% to 10 wt% [19].

2.2 Carbon Black

Carbon black (CB) is a material that has found extensive use in a number of application. It consists mostly of element of carbon, and it is in form of spherical particle that have been fused together to form aggregates that are classically around 30-100 nm in size. CB is generally used as a reinforcing filler to improve dimensional stability, a conductive filler, an ultraviolet light stabilizer, an antioxidant to prolong the lifetime of rubber, and a pigment or colorant. CB is an amorphous form of carbon with a structure comparable to disordered graphite. When aromatic hydrocarbons are subjected to partial combustion at high temperature their molecules will dissociate through the rupture of C H bonds. Afterward, carbon atoms

and aromatic radicals react to form layer structures composed of hexagonal carbon rings, which tend to stack in three to four layers, forming crystallographic structures. Crystallites then form primary particles, which further fuse into primary aggregates. Van der Waals forces cause these aggregates to join in more loosely collected agglomerates [20, 21].

There are five types of CBs manufactured in the CB manufacturing: furnace black, thermal black, lampblack, channel black and acetylene black. Different processes produce different products with various physical and chemical properties. The most usually used CBs in rubber and plastics applications are furnace and thermal blacks. Over 90% of the CBs presently produced are made by the furnace process, in which oil is thermally decomposed to form CB particles. Only CBs with small diameter and large surface area are appropriate as the filler to improve electric conductivity [20].

Basic Information on Carbon Black [19, 21]

Production: CB results from partial combustion or thermal cracking of a hydrocarbon raw material (Figure 2.2). Currently almost all CBs are manufactured by the oil furnace process: a highly aromatic feedstock is incompletely burned by atomization into a hot flame made of natural gas and preheated air, the reactor temperature attainment more than 1500°C. At the process end, powder ("fluffy") or pelletized CB is assembled. The oil furnace process permits effective control of end product physical and chemical properties.

$$C_xH_x + O_2 \xrightarrow{heat} C + CH_4 + CO + H_2 + CO_2 + H_2O$$
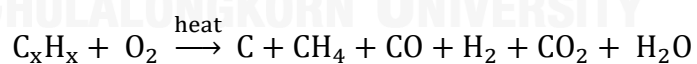
Figure 2. 2: Partial oxidation of aromatic hydrocarbons.

Form: CB is a particulate form of industrial carbon at which shows a "quasi-graphitic" microstructure (Figure 2.3). The manufacturing process leaves various forms of oxygenated groups on carbon black layer planes: mostly phenolic, quinolic and carboxyl chemisorbed complexes. During the nucleation process (Figure 2.4), three to four layers form crystallites, which combine to form primary particles and continue to grow into aggregates. Agglomerates are a dense assembly of aggregates formed

due to the small distances between them and the strong van der Waals forces present. CB dispersion in a polymer matrix will need the breaking of these links. An aggregate is indivisible and represents the CB "base unit" although a CB is frequently characterized by its primary particle size. In summary, the finer the prime particles, and subsequently the smaller the aggregates, the lower will be the level of electrical resistivity when dispersed in polymer matrix.
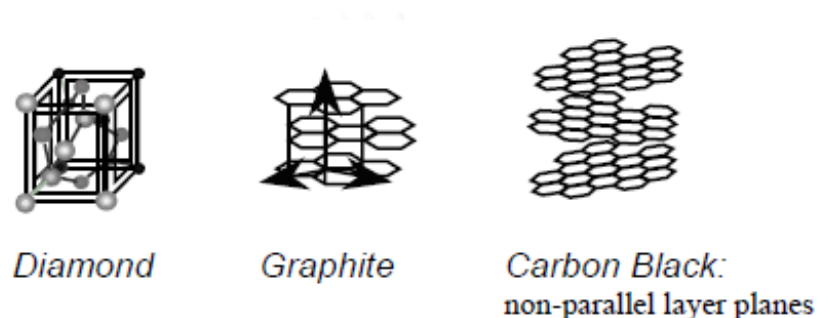
Figure 2. 3: CB "quasi-graphitic" microstructure compared to the two regular crystalline forms of carbon (diamond and graphite) [19].

Fundamental Properties of Conductive Carbon Black

Particle Size: Electron microscopy shows CB to be composed of clusters of spherical primary particles, called aggregate or primary aggregates (see Figure 2.4).
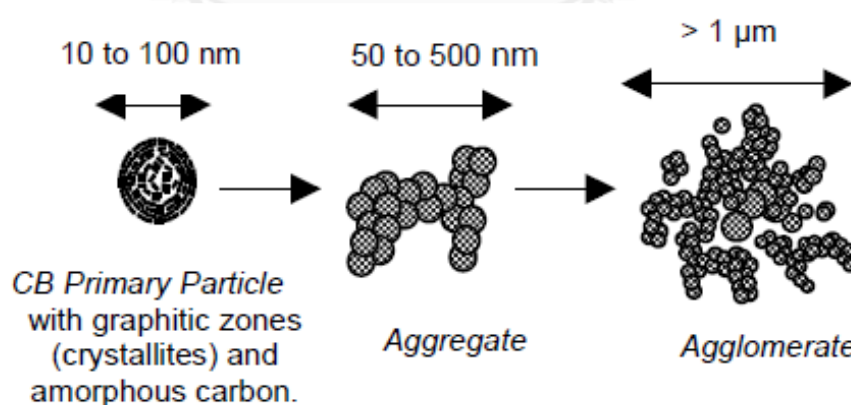
Figure 2. 4: CB primary particles fuse together in the reactor and form aggregates and agglomerates [19].

Structure: All methods for structure valuation are indirect and essentially consist of measuring the absorbed amount of a suitable chemical, for instance dibutyl

phthalate DBP. Consequences are expressed in ml or cm^3 (of DBP) absorbed per 100 g of filler. Structure or the DBP adsorbed is function of the aggregates void volumes and defines the degree to which the CB particles have fused together to form aggregates: a low structure CB (low DBP) is made of few primary particles compactly fused together while a high structure CB (high DBP) is made of many primary particles with considerable branching and chaining (see Figure 2.5).
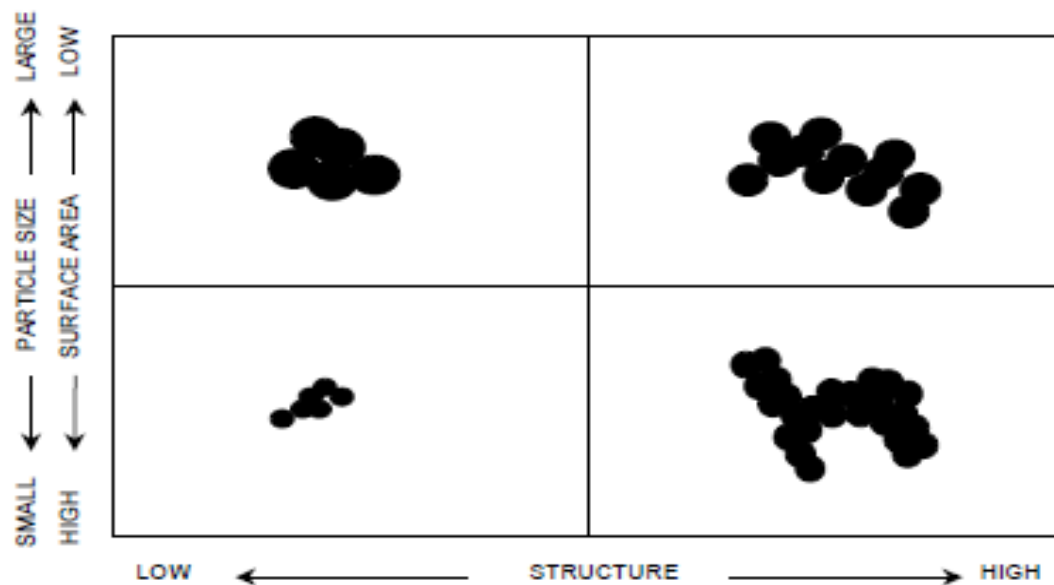
Figure 2. 5: Visualization of CB particle size /surface area and structure [19].

Surface area: The specific surface area is evaluated either through iodine I_2 adsorption (result is given in mg of I_2 per g of CB), or through nitrogen N_2 adsorption (result in m^2/g of CB. Small particles will discuss a high surface area per unit weight so the high surface area is the critical characteristics of CBs that inform electrical conductivity at lower contents in polymer composites.

According to the CB aggregate structure, CBs are categorized into a high structure and a low structure [20]. High structure CB is characterized by additional branching and chaining per primary aggregate compared to the low structure CB. The main disadvantage of the low structure CB-filled polymer composites is the high concentration of CB (~15–20 wt%) required to attain the percolation threshold. Such high filler loading affects the composite mechanical properties, processability and

increases the price of the final composite. Consequently, reducing CB content in conductive polymer composites is a key research challenge. Recently, one of the most common methods to decrease the percolation threshold and electrical resistivity at a relatively low CB content is to use two-component polymer blends as matrix based on the ''double percolation'' behavior, i.e. the percolation of electrical conductivity in such an immiscible or partially miscible polymer blend depends on the continuity of CB-rich phase or the interface as well as the percolation of CB in CB-rich phase or at the interface. By the preferential localization of CB particles in a distinct region, such as a phase of a dual continuous phase blend or interface between two phases, the effective CB loading was greatly higher than its nominal value, hence the percolation threshold reduced significantly [22].

2.3 Mechanism of Electrical Conductivity

Basic behavior

In the area of low filler volume fraction, the conductive filler particles of different sizes and shapes are dispersed homogeneously into the insulating matrix. Consequently, there are no contracts between the adjoining filler particles. As the volume fraction of the filler increases, particles come closer and small agglomerates begin to growth. In certain volume fraction i.e. percolation threshold, conducting particles or small agglomerates touches other agglomerates or particles and forms a conductive network inside the conducting particles as shown in Figure 2.6.
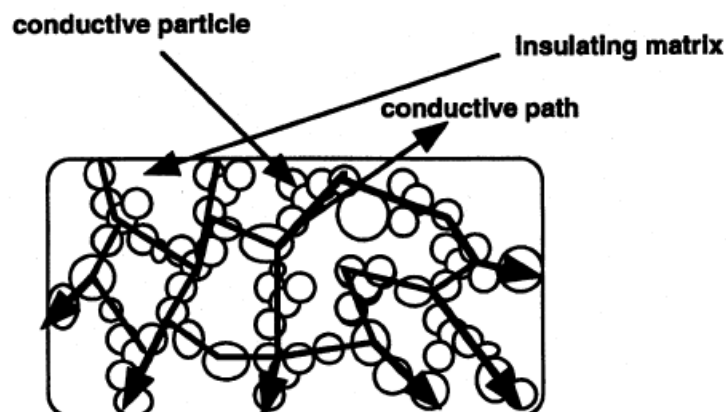
Figure 2. 6: Conductive paths in composites without pressure [23].
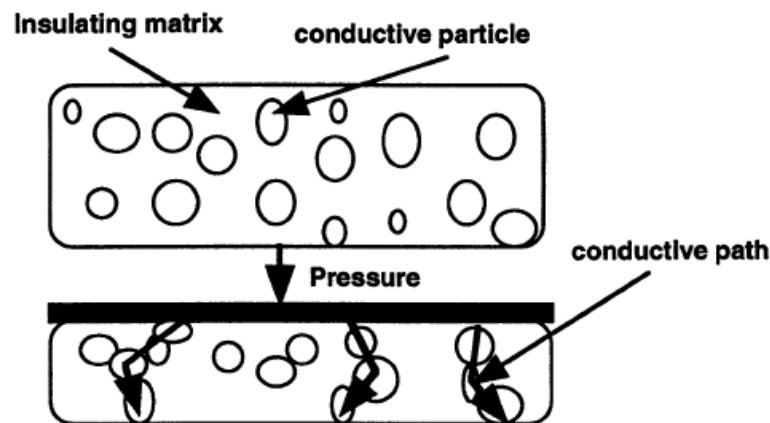
Figure 2. 7: Formation of conductive paths in composite by pressing [23].

Effect of pressure on resistivity measurement

The electrical resistance of conductive filler dispersed polymer composite materials depend mostly on applied stress, magnetic field, temperature and humidity. As explained above, at a certain volume fraction of filler, the conductive path is formed in an insulating matrix when the conducting particles come in contact with another and form one to three dimensional conducting network structure. Nevertheless, when pressure is applied on the composite, the conducting particles originate contact with one another more readily and a conducting path is formed. When the pressure is released, the conducting path is discontinued. The formation of conductive pathways after applying external pressure is shown in Figure 2.7. When the pressure is applied, the conducting path is formed when the volume fraction of filler is less than that of composites without applied pressure i.e. total volume of the matrix declines upon pressure.

2.4 Percolation Theory and Models

Polymers are generally an insulating material. By adding electrically conductive fillers, the composites will display electrical conductivity and can used in a variety of applications. The electrical conductivity of the mixture increases intensely at a critical filler concentration called the percolation threshold. Below this concentration the filler particles are not consistent within the polymer matrix. The

composite remains an insulator with no contact between the filler particles. Once the concentration reaches the percolation threshold concentration, the filler particles are able to contact each other, and form a conducting network. Figure 2.8 displays typical electrical conductivity behavior of a polymer filled with conductive filler as a function of filler concentration. It is valuable to note that the theoretically expected percolation threshold for a randomly dispersed system is around 15 vol% [24]. Many models and equations have been offered to understand this behavior. Some of these models are reviewed in this section.
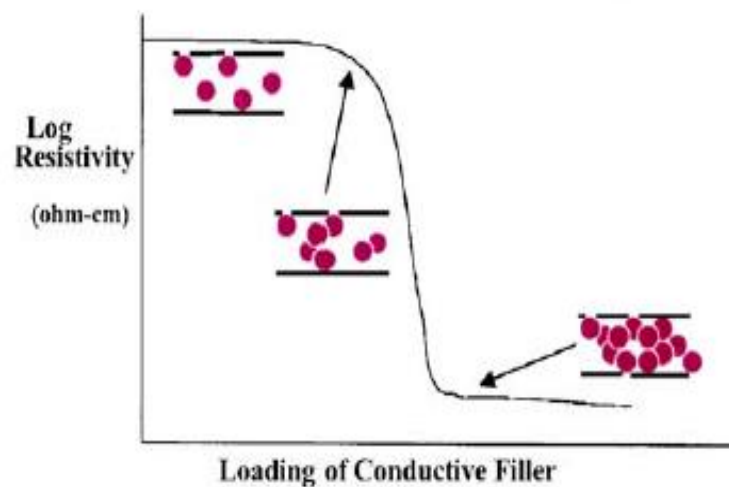
Figure 2. 8: Schematic of electrical resistivity as a function of filler loading [24].

Kirkpatrick formalized percolation theory to predict resistivity above the percolation threshold concentration [20, 23]. He showed that electrical resistivity follows the power-law correlation:

$$\rho = \rho_0(V - V_c)^{-s} \qquad (2.1)$$

where ρ is the composite electrical resistivity (Ω cm), ρ_0 is the intrinsic resistivity of the filler (Ω cm), V is the volume fraction of the filler, V_c is the percolation threshold, and s is the power-law exponent. The value of s is typically between 1.5 and 3 for three-dimensional percolation.

2.5 Minimization of CB Loading by using Polymer Blend as Matrix

In terms large-scale practical applications, melt processing, the addition of CB in the single thermoplastic polymeric hosts is interested. However, in most of these systems, V_c remains high because of the high filler content. This system leads to difficulties in processing due to an increase in melt-viscosity of the blends, the high final cost and, poor mechanical properties, such as brittle. It is necessary for the conducting filler content to be as low as possible to achieve good processability, low cost, and good mechanical properties. The general approach undertaken to reduce to CB content is by formation of segregated CB structures. Therefore, the dispersion of CB particles in a semi-crystalline polymer, where the CB is localized in the amorphous regions, results in a percolation threshold decrease. Otherwise, binary immiscible or partially miscible blend have been currently received and interest to be utilized in minimizing percolation threshold since heterogeneous morphologies allow the filler preferentially accumulate in certain regions. To attain isotropically conductive materials, multiphase systems, which allow filler to form conductive network within continuous phase are preferred.

The selective localization of conducting particles in one of the two phases or at the interface of a co-continuous two-phase polymer blend is a very efficient strategy to decrease the CB percolation threshold [25] (see Figure 2.9, for example). It is worth pointing out that double percolation or percolation-within-percolation is at the original of this location:

- percolation of the polymer phases and thus of their interface and
- percolation of the conductive particles in one phase or at the interface

<div align="center">(a)   (b)</div>
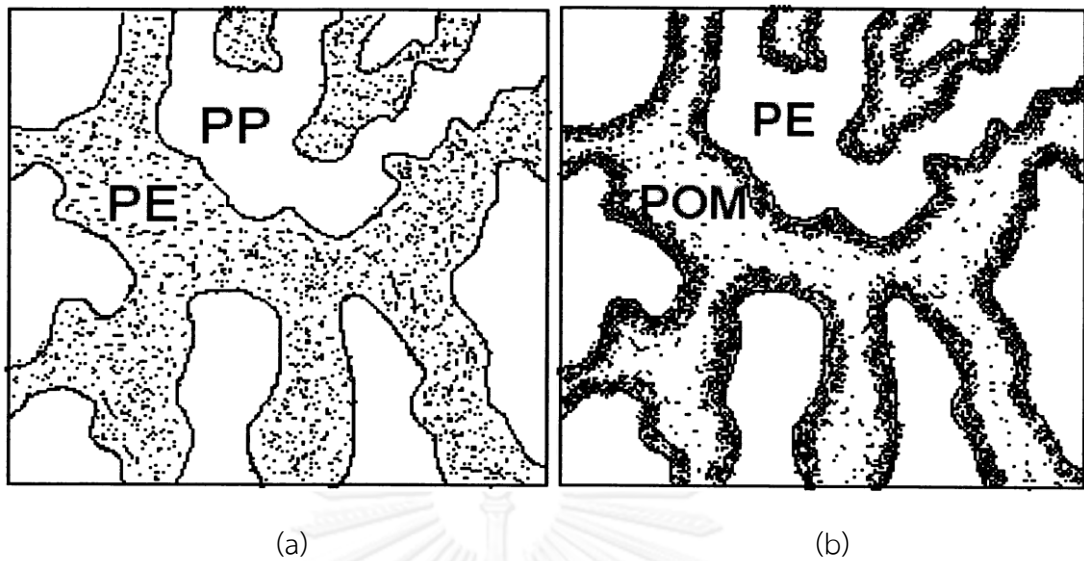
Figure 2. 9: Self-assembly structure model of polymer PE/PP blend and PE/POM blend filled with carbon black: (a) CB filled in one phase (PE), (b) CB filled in interface [25].

The existence of different CB arranges is given by the following factors [26-28]:

1. Thermodynamic factor: relate between interface tension polymer A-filler, polymer B-filler and polymer-polymer. When CB particles blended with the polymer blends consisting of polymers A and B, phase where CB located is predicted by Young's equation:

$$\omega = \frac{(\gamma_{CB-A} - \gamma_{CB-B})}{\gamma_{A-B}} \qquad (2.4)$$

where γ_{CB-A}, γ_{CB-B} and γ_{A-B} are, respectively, the interfacial energy between polymer A and CB, between polymer B and CB, and between polymers. ω is called the wetting coefficient. When

$\omega > 1$ CB particles distribute within the A phase

$-1 < \omega < 1$ CB particles distribute at the interface

$\omega < -1$ CB particles distribute within the A phase

In principle the knowledge of the polymer/polymer and of the polymer/filler interfacial tensions should be sufficient to anticipate the morphology. Nevertheless, if experimental data may be found for polymer/polymer interface it is almost difficult to find it for polymer/filler. Generally, they are estimated with the help of theoretical models like the well-known Wu equations [29]:

$$\gamma_{12} = \gamma_1 + \gamma_2 - 2\sqrt{\gamma_1^d \gamma_2^d} - 2\sqrt{\gamma_1^p \gamma_2^p} \qquad (2.5)$$

Only γ_i, the surface tension of component i need to be known. The exponents d and p stand for respectively the dispersive and the polar contribution to the surface tension.

2. Kinetic factor: relate between viscosities of the polymer components at the temperature of processing. The CB particles prefer to localize in low viscosity polymer phase.

Mamunya et ai. [26] studied the percolation phenomena in polymers containing dispersed iron. In this research, he explained that the differences are caused by the specific structure of the composite based on the PE/POM blend. Due to the large difference between the polymer melt viscosities of FE and POM (melt flow indexes 1.6 and 10.9 g/10 min, respectively), the filler is located in the POM phase during formation of the filled system from polymer melt in the extruder. So the Fe particles in the PE/POM/FE composite will be selectively dispersed in the PE phase because of its lower viscosity as shown in Figure 2.10.
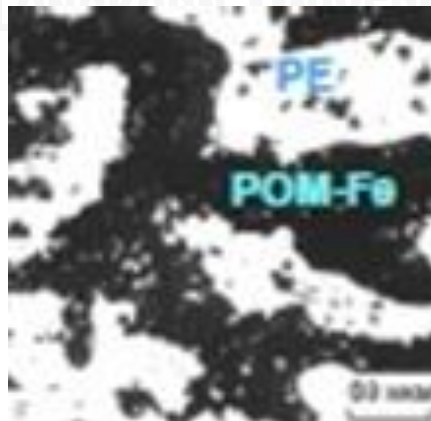
Figure 2. 10: Optical microscopy micrographs of the PE/POM-Fe composite [26].

3. Processing factor: relate methods of the filler introduction to the complex polymer matrix, which can either enhance or depress influence of thermodynamic and kinetic factors. Generally, filled polymer blends can be prepared by the following five methods [25]:

Method 1 -4 are two-stages; Method 5 is one-stage.

Figure 2. 11: Five methods to introduce filler.

It has been reported that the processing sequence is one of the important factors that influence the electrical properties of CB-filled various binary polymer blends [30]. Cui et al. [31] studied the effect of processing sequence on the electrical properties of immiscible PP/novolac blends filled with CB. The effect of different processing sequence on the electrical properties was investigated. In addition to the simultaneously melt-mixing blends, (Novolac+CB)/PP and (PP+CB)/Novolac blends were prepared by pre-melt mixing CB with Novolac resin (or PP), followed by the addition of PP (or Novolac resin). Table 2.1 displays the volume resistivity of PP/Novolac/CB (70/30/6) blends with different processing sequence. For the PP/Novolac/CB (70/30/6) blends, the volume resistivity of the simultaneously melt-blended and the (Novolac+CB)/PP samples is alike. While the volume resistivity of

the (PP+CB)/Novolac samples are much higher (2.0×10^{16} Ω cm). It could be conclude that the addition of Novolac into PP/CB increased the volume resistivity. It proposes that the CB particles partially migrate into the Novolac phase, reducing the CB concentration in the continuous PP matrix. It could be a good attraction of Novolac with CB and the strong Novolac/CB interaction that drive CB to interact with the Novolac phase and removal to it.

Table 2. 1: Volume resistivity of PP/Novolac/CB (70/30/6) blends with different processing sequences [31].

Sample Composition	Method of Processing	Volume Resistivity (Ω·cm)
PP/Novolac/CB (70/30/6)	Simultaneously melt-blended	7.1×10^{8}
	(Novolac+CB)/PP	4.7×10^{8}
	(PP+CB)/Novolac	2.0×10^{16}

CHAPTER III

LITERATURE REVIEWS

Foulger 1999 [32] studied the reduced percolation thresholds of immiscible conductive blends. The effect of CB content on the volume resistivity of the HDPE/CB, EVA/CB and EVA/HDPE/CB is shown in Figure 3.1. The EVA/CB composites do not exhibit in the same manner as the HDPE/CB composites, the drop in volume resistivity at a well-defined threshold of incorporated CB, but instead exhibit a sloping drop in volume resistivity between the unfilled EVA up to 18 wt% of combined CB. At CB contents greater than 18 wt%, the rate in decrease of volume resistivity with increasing CB content is reduced. Furthermore, the EVA/CB composites have a significantly higher volume resistivity, relative to the HDPE/CB system, at CB concentration levels past the HDPE/CB percolation threshold. A contributing factor to the large disparity in the conductivity characteristics of these systems is the relative difference in the surface tension and polarity of the polymers. EVA is characterized by a higher surface tension and polarity compared to that of HDPE, both of which have been shown to promote higher CB percolation thresholds. The percolation threshold of HDPE/CB was observed at 6-12 wt% CB The percolation threshold of the EVA/HDPE/CB composites is between 3.6 and 4.2 wt% CB where the volume resistivity changes by 8 orders of magnitude. This threshold is at a significantly lower CB content than the individually filled HDPE or EVA. From the results, it could be concluded that the usage of polymer blend can be reduced CB in composites.
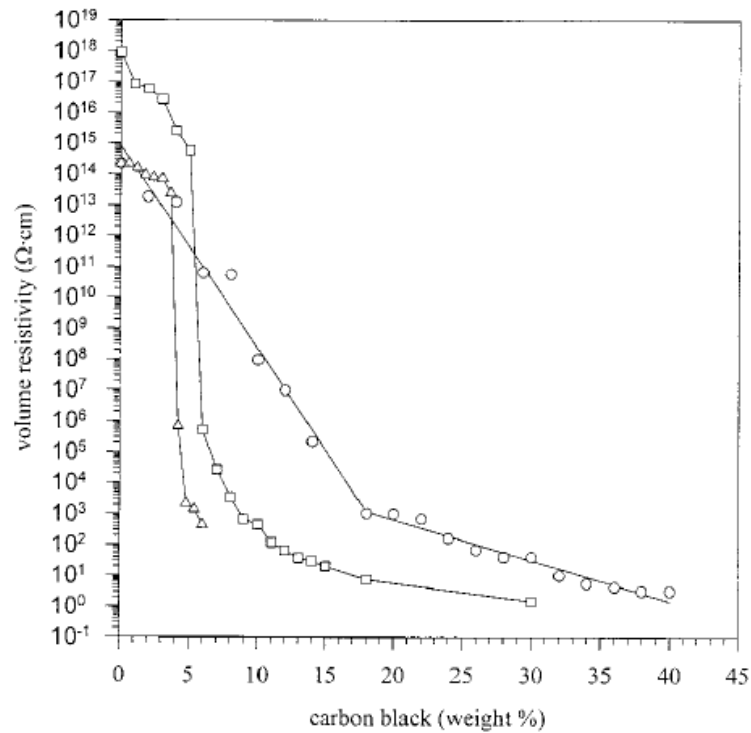
Figure 3. 1: Volume resistivity of EVA/HDPE/CB composites (Δ), HDPE/CB composites ($\square$), and EVA/CB composites (O) [32].

Farshidfar et al. 2006 [11] were found that high density polyethylene (HDPE)/ethylene-propylene-diene monomer (EPDM) blend ratio (70/30) has lower percolation threshold and volume resistivity than individually carbon black filled HDPE and EPDM due to "double percolation" effect. Carbon fibers were also added to the polymer-carbon black mixtures to enhance the conductivity. The electrical conductivity of composites with different ratios of carbon black (CB) content to carbon fiber (CF) content was studied. The CB content is the main factor to determine the resistivity of the composites filled with CB and CF. The result of the filler effect on the resistivity of the composites is shown in Table 3.1.

Table 3. 1: Variation of the resistivity of the composites containing 80% polymer (HDPE/EPDM: 70/30) and 20% conductive filler [11].

Carbon black (wt%)	Carbon fiber (wt%)	Volume resistivity (Ω.cm)
20	0	2.72
0	20	15.3
5	15	0.86
15	5	0.55

The effect of EPDM contents on HDPE/EPDM/CB composites, different mixtures of HDPE and EPDM with 5 wt% CB were prepared and the resistivity results are shown in Table 3.2. According to the data in Table 3.2, the resistivity values measured from these composites are sensitive to blend composition. Increasing the EPDM content in the blend will lead to the decrease in volume resistivity and after reaching to a specified content then resistivity increases as the concentration of EPDM is increased further.

Table 3. 2: Variation of the resistivity of 5wt% CB-filled HDPE/EPDM mixtures [11].

HDPE (wt%)	EDPM (wt%)	Volume resistivity (Ω.cm)
90	10	6.0×10^2
70	30	4.2×10^2
45	55	3.0×10^2
40	60	1.6×10^6

In accordance with the results of Chan et al. 1997 [33], the higher viscosity of EPDM is anticipated to promote filler localization at the HDPE-EPDM interface, whereas the lower viscosity of HDPE may help to connect CB channels throughout the entire composite volume. Thus, a combination of the clearly different melt-flow properties of these polymers may synergistically achieve higher conductivity than that of the constituent polymers. In one article by Sumita et al. [34] dispersion of CB and electrical conductivity of polymer blends were discussed. There are two Types of heterogeneous distribution of CB in filled Polymer blends. One is predominantly distributed in one phase of the blend, and the other is distributed at the interface of two polymers. If CB is distributed at the interface, the envelope formation of CB particles around the dispersed phase makes the conductive paths more effective than the single matrix.

Shen et al. 2012 [13] studied the combined effects of CB and CF on the electrical properties of composites based on polyethylene or polyethylene/polypropylene blend. These composites were mixed with one (CB) or two fillers (CB and CF). For the two filler composites, the CF content was fixed at 2 wt%, which is too low to form a conductive network. For the HDPE/PP based composite mixed with CB and CF, the weight ratio of HDPE to PP is 60/40. Since the volume fraction of HDPE is greater than 50%, the HDPE matrix forms a continuous phase.

Figure 3.2 (a) and (b) shows that compared with HDPE/CB and HDPE/PP/CB composites, the volume resistivity of HDPE/CB/CF and HDPE/PP/CB/CF decreased up to 3.0 and 11.2 orders of magnitude, respectively, at the same total fillers concentration after the addition of 2 wt% CF. This figure shows that the percolation regions of the HDPE/PP based composites are narrower than those of HDPE-based composites and they are shifted to the left. The HDPE/CB/CF and HDPE/PP/CB/CF composites have similar percolation regions to the HDPE/CB and HDPE/PP/CB composites, respectively. This finding indicates that percolation depends to a greater degree on the CB content than on the CF content, because the CF content is insufficient for the formation of a conductive network by itself. However, the filler

content where percolation commences is lower in the polymer blend composite than in the single semicrystalline polymer composite. This is due to double percolation occurring due to the conductive filler having a heterogeneous distribution in one phase of the blended matrix.
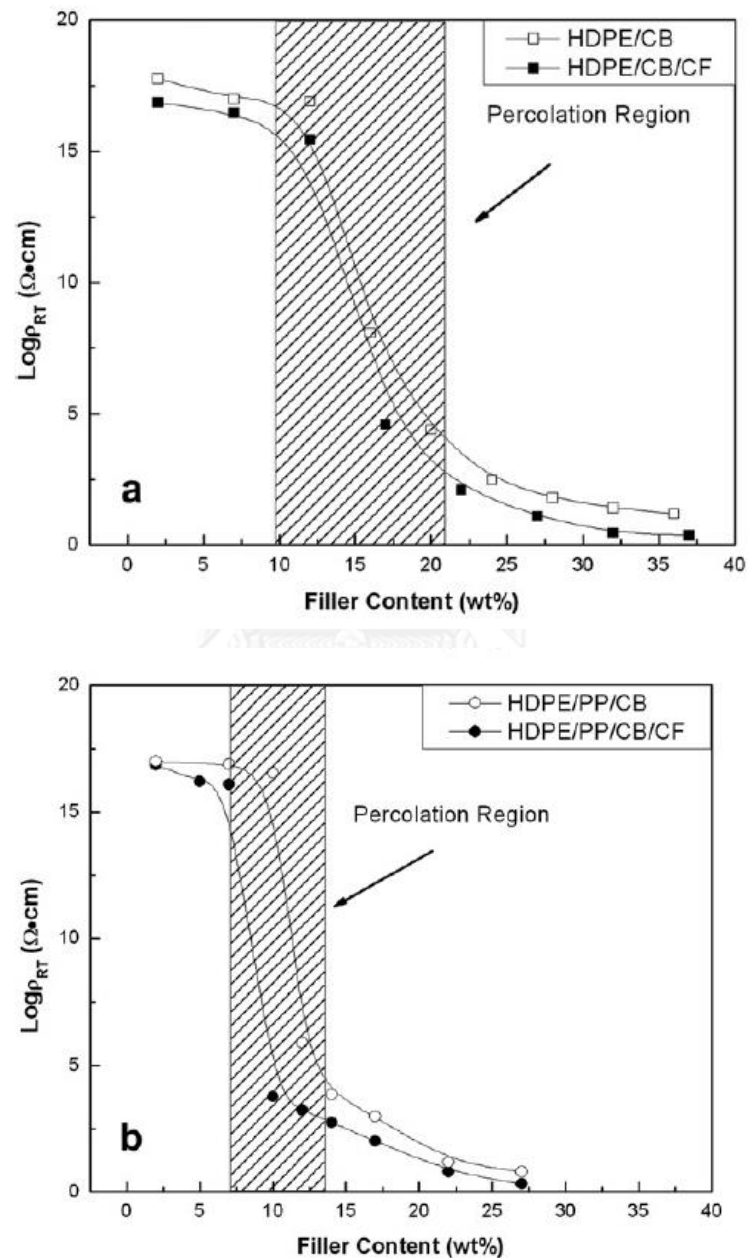
Figure 3. 2: Resistivity as a function of total fillers concentration for (a) HDPE-based and (b) HDPE/PP-based composites. The CF content is fixed at 2 wt% [13].
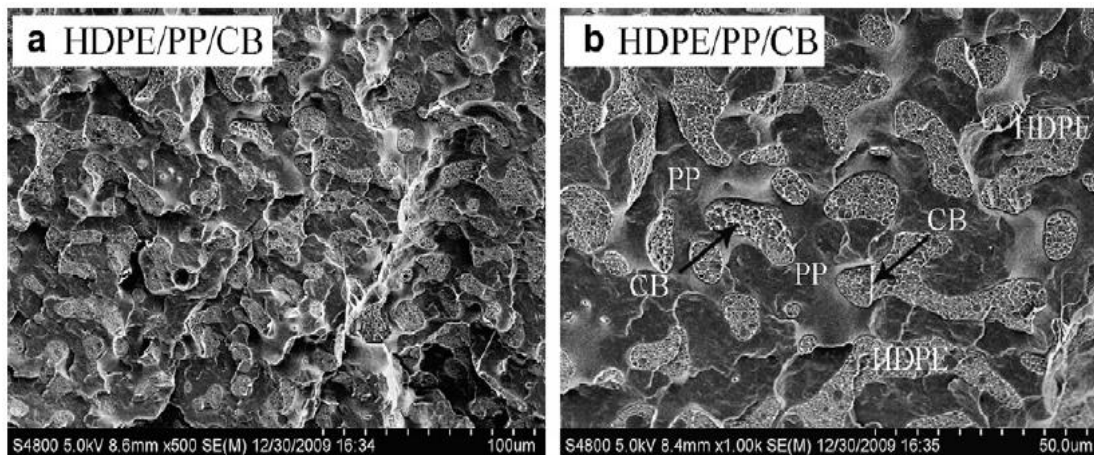
Figure 3. 3: SEM images at different magnifications ((a) ×500 and (b) ×1.00K) of the fracture surface of HDPE/PP-based composite mixed at 5 wt% CB, where the CB particles are located in HDPE phase [13].

The SEM micrographs in Figure 3.3 (a) and (b) show two distinct phases: one that contains CB particles (the HDPE phase) and another that is free of CB particles. Both HDPE and PP form continuous phases; such structures are known as co-continuous phase structures. When the volume fraction of CB particles distributed in the HDPE phase extends to the percolation threshold of the HDPE/CB composite, a network of conductive chains forms in the HDPE phase. For the polymer blend composites, the distribution of CB in a phase is generally determined by the interfacial free energy [35]. Zhang et al. calculated the interfacial free energies of PP/CB (γ_{PP-CB} = 4.1 mJ/m^2) and of HDPE/CB (γ_{PE-CB} = 2.2 mJ/m^2). Therefore, the CB particles in the HDPE/PP/CB composite will be selectively distributed in the HDPE phase because of its lower interfacial free energy. Therefore, the co-continuous structure of immiscible or partially miscible blend can markedly reduce the percolation threshold. Additionally, it may deliver supplementary advantages associated with co-continuous structure, i.e., contribution of properties of both polymers, high flow, toughness/ductility and processability [6-13].

Using CB as an additive to attain electrical conductivity generally requires a concentration so high that it will increase the melt viscosity and decrease the mechanical properties of the polymers. One of the recent trends is to use multiphase polymer blends to decrease the amount of conductive fillers in composites [7, 33]. The result of adding a second immiscible polymer blend into a polymer/CB blend is shown in Table 3.3 [20].

Table 3. 3: Effects of PP on properties of PC/CB blends [20]

Composition PC/CB/PP (wt%)	Tensile Strength (MPa)	Tensile Elongation (%)	Impact strength (J/m)	Viscosity at 100 s^{-1} (Pa s)
100:0:0	59.3	229	1221	1735
95:5:0	63.4	20.2	525	2160
90:0:10	44.4	142	850	611
85:5:10	49.1	14.1	354	756
80:0:20	41.8	37.8	593	320
75:5:20	43.0	12.8	380	510

The table compares the effect of adding PP on the apparent viscosity and several mechanical properties of PC/CB blends. It can be seen that adding CB into PC increased the tensile strength and melt viscosity but decreased tensile elongation and impact strength. Adding PP and other polyolefin can decrease the viscosity of the mixture even when the polyolefin has a higher viscosity than the PC. This happens because the melt viscosity of PC/PP blends belongs to the negative deviation type and slip at the interface between the two phases is expected during the flow.

U. S. Pat. No. 6,331,586 [36] claims (1) a conductive polymer blend comprising: (a) at least two polymers which are at least partially immiscible with each other, and are present in proportions such that each polymer forms a respective continuous phase and the two continuous polymer phases are co-continuous with each other in the polymer blends; and (b) at least one conductive material in particulate or fiber form which is durably localized in one of said co-continuous polymer phases or durably localized at a continuous interface between said co-continuous polymer phases, wherein said at least two polymers are a pair selected from the following pairs of polymer: HDPE/TPU, HDPE/EPR, HDPE/EPDM, HDPE/mLLDPE, PP/EPDM, PP/EPR, mLLDPE/EPR.

A conductive polymer blend according to claim (1), wherein said conductive polymer forms a product which retains at least about 65% of the elongation at break of the polymer in the blend which has the highest elongation at break, as compared to the other polymers in the blend, if each polymer were used as a single-phase polymer system and formed into a product under the same conditions.

Naiki et al. [37] studied tensile elongation of PP/EPR blends. These blends are shown the temperature dependence of E' and E'' of PP1/EPR2 (EPR2, Mw = 320,000) and PP1/EPR4 (EPR4, Mw = 200,000) blends (Figure 3.4). Interpretation of the dynamic mechanical analysis of the PP/EPR blends has been well described. The decreases in E' at about -40 and 10 °C were attributed to the glass transitions of EPR and PP, respectively. The appearance of the glass transition of each component in the blends implies that these blends were phase-separated systems. For binary systems, the immiscible blend can be designed in a way that favors the dispersion of CB particles in the minor component of a co-continuous blend. Stress–strain curves of PP and PP1/EPR2 and PP1/EPR4 blends are shown in Figure 3.5. The Young's moduli were lowered by the addition of EPR to PP. The elongation to rupture usually increased with increasing MW of EPR. Therefore, toughness of PP has been improved by blending it with elastomer such as EPR.
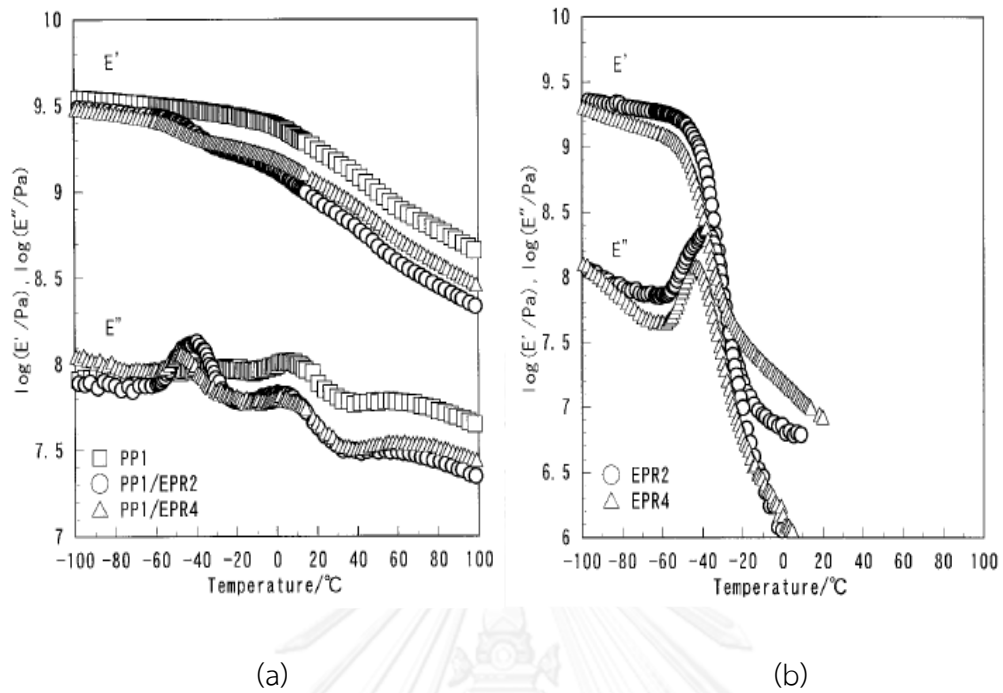
Figure 3. 4: Temperature dependence of E′ and E″ for (a) PP1 and PP1/EPR blends and (b) EPR [37].
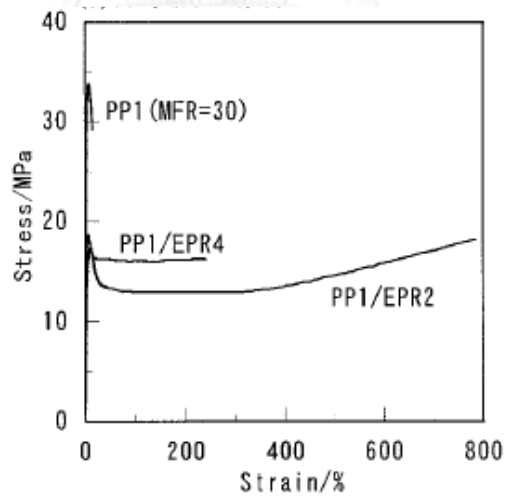
Figure 3. 5: Stress–strain curves for PP and PP/EPR blends ratio (70/30) at 23°C [37].

CHAPTER IV

EXPERIMENTAL

4.1 Materials

Polypropylene (PP, 1102H) and Ethylene propylene rubber (EPR, 3325M) were produced by IRPC Co., Ltd., Thailand, with a melt flow index (MFI) of 2 and 9 g/10 min (230 $^{\circ}$C, 2.16 kg), respectively. Electrically conductive CB (ENSACO$^{\circledR}$ 250) was provided by TIMCAL Co., Ltd., with DBP absorption of 190 ml/100 g, specific surface area of 65 m^2/g, and mean particles diameter of 45 nm.

4.2 Sample Preparation

Melt mixing of CB-filled PP/EPR blends was carried out by an internal mixer (Figure 4.1) at 200°C and 40 rpm for 10 minutes. PP, EPR and CB were dried at 80, 80 and 110°C, respectively for 24 hours in an oven in order to remove moisture. PP/EPR blends were melt mixed at the weight ratios ranging from 100/0 to 50/50 with CB as conductive filler ranging from 0 to 30 wt% in the internal mixer. Blends were formed by compression molder (Figure 4.2) at 15 MPa and 200 $^{\circ}$C in a mold 120 × 120 × 2 mm^3 for 10 min. After being cooled to near room temperature in air, the composite sheets were removed and cut into test samples.

Figure 4. 1: Internal mixer.

Figure 4. 2: Compression molder.

4.3 Characterization Methods

4.3.1 Differential Scanning Calorimetry (DSC)

The melting temperature of PP/EPR blends were examined by using a differential scanning calorimeter (DSC) model 2910 from TA Instrument. For each test, a small amount of the sample ranging from 8-10 mg was placed on the aluminum pan and sealed hermetically with aluminum covers. The experiment was done using a heating rate of 10°C/min to heat the sealed sample from 45°C up 200°C under N_2 purging. The purge nitrogen gas flow rate was maintained to be constant at 50 ml/min. The processing temperature, time and glass transition temperature were obtained from the thermograms while the percentage of resin conversion was calculated from the DSC thermograms.

4.3.2 Density Measurement

The density of each specimen was determined by water displacement method according to ASTM D 792 (Method A). All specimens were prepared in a rectangular shape (50 mm × 25 mm × 2 mm). All specimen was weighed in air and in water at $23 \pm 2^{\circ}$C. The density was calculated using Equation (4.1). An average value from at least five specimens was calculated.

$$\rho = \left[\frac{A}{A-B}\right] \times \rho_0 \qquad (4.1)$$

where
ρ = density of the specimen (g/cm^3)

A = weight of the specimen in air (g)

B = weight of the specimen in liquid (water) at $23 \pm 2^{\circ}$C (g)

ρ_0 = density of the liquid (water) at the given temperature (g/cm^3)

The measurement was carried out using five specimens per formulation and the average value of the sample was obtained.

4.3.3 Dynamic Mechanical Analysis (DMA)

Dynamic mechanical analyzer (DMA) model DMA242 from NETZSCH Instrument was used to investigate dynamic mechanical properties. The dimension of specimens was 50 mm $\times$ 10 mm $\times$ 2.0 mm (W$\times$L$\times$T). The test was performed under the three-point bending mode. A strain in the range of 0 to 30 μm was applied sinusoidally at a frequency of 1 Hz. The temperature was scanned from -50 $^{\circ}$C to 80 $^{\circ}$C with a heating rate of 2 $^{\circ}$C /min under nitrogen atmosphere. The glass transition temperature was taken as the maximum point on the loss modulus curve in the temperature sweep tests. The storage modulus (E'), loss modulus (E''), and loss tangent (tanδ) were then attained. The glass transition temperature (T_g) was taken as the maximum point on the loss modulus curve in the DMA thermograms.

4.3.4 Rheological Property Measurement

Rheological properties of neat PP and EPR were examined by using Rheometer (Haake Rheo Stress 600, Thermo Electron Cooperation) equipped with 25 mm parallel plate geometry. The measuring gap was set at 1 mm and the experiment was performed under a dynamic frequency sweep mode using frequencies ranging from 0.1 to 100 Hz at constant temperature 200°C. All samples are preheat for 5 minutes before testing.

4.3.5 Electrical Property Measurement

Electrical resistivity measurements were conducted using two different instruments. At least three samples were tested for each formulation. An Electrometer (4284A, HP) was used to perform room-temperature resistivity measurements on samples with resistivity lower than 10^6 Ω cm, while a high-resistance meter (6517A, Keithley) was used for samples with higher resistivity. An average electrical resistivity value from of about 3 readings was reported. All samples are tested under a voltage of 2 V.

4.3.6 Tensile Property Measurement

Tensile properties of the PP/EPR/CB composite specimens were determined utilizing a Universal Testing Machine model 5567 from Instron Instrument according to ASTM D638. The test specimens were a dumbbell (dog bone) shape with a uniform thickness, which were prepared by an injection machine. They were tested by using a cross-head speed of 50 mm/min with the pre-load of 10 N giving a straight tensile force. The tensile strength value defined as the stress at yield or at break whereas the tensile modulus values were determined by the ratio of stress to strain that was determined from the initial slope of the stress-strain curve. Five specimens from each formulation were tested and the average values were reported.

4.3.7 Notched Izod Impact Testing

Notched Izod impact is a single point test that measures a materials resistance to impact from a swinging pendulum. The impact is defined as the kinetic energy needed to initiate fracture and continue the fracture until the specimen is broken. Notched Izod impact strength was measured by an impact tester from Yasuda Seiki Seisakusho Ltd. (Japan) according to ASTM D256. The specimens were prepared by injection molding machine. The impact bar specimen had a length of 63 mm, a width of 12.7 mm, and a thickness of 3 mm. A notch at one side centered in the direction along the length with a depth of 2 mm was made for each specimen.

4.3.8 Melt Flow Index Measurement

Melt flow index or MFI is a measure of an ease of flow of the melt of PP/EPR/CB composites using a melt flow indexer (Model 1 GOTTFERT). It is defined as the mass of polymer, in grams, flowing in ten minutes through a capillary of an orifice with a diameter of 2.095 mm and orifice length of 8.0 mm according to ASTM D 1238 standard at 230°C/2.16kg load. All samples are preheat for 3 minutes before testing. Two specimens from each formulation were tested and the average values were reported.

4.3.9 Thermogravimetric Analysis (TGA)

Thermogravimetric analyzer model TGA1 from Mettler Toledo (Germany) was used to investigate degradation temperature (T_d) and char yield of PP/EPR/CB composites. The initial mass of the composite to be tested was about 10-15 mg. It was heated from room temperature to 800°C at a heating rate of 20°C/min under nitrogen purging with a constant flow of 80 ml/min. The degradation temperature at 5% weight loss and solid residue of each specimen determined at 800°C were recorded for each formulation.

4.3.10 Scanning Electron Microscope (SEM)

Scanning electron microscope (SEM) model JHM-5410LV from JEOL was used to investigate phase morphology of PP/EPR blends and PP/EPR/CB composites at an acceleration voltage of 15 kV. All specimens were coated with thin film of gold using a JEOL ion sputtering device (model JFC-1100E) for 2 min to obtain a thickness of approximately 10-20 nm and the micrographs of the freeze-fracture surface were taken. The obtained micrographs were used to evaluate the selective distribution of CB in PP/EPR blends.

CHAPTER V

RESULTS AND DISCUSSION

5.1 Density Measurement of CB-Filled PP/EPR Blends

Density measurement of CB-filled PP/EPR blends was performed to examine the presence of void in the specimens. The densities of PP/EPR blends at the weight ratios ranging from 100/0 to 50/50 with CB as conductive filler ranging from 0 to 30 wt% comparing with their theoretical densities are shown in Table 5.1. The densities of PP/EPR/CB composites are determined experimentally by water displacement method (ASTM D792) and Equation (5.1) by averaging the value from seven specimens whereas the theoretical densities of the PP/EPR/CB composites were calculated from Equation (5.2).

$$\rho = \left[\frac{A}{A-B}\right] \times \rho_0 \qquad\qquad (5.1)$$

Where

ρ = Measured density of the specimen, g/cm^3

A = Weight of the specimen in air, g

B = Weight of the specimen in liquid, g

ρ_o = Density of the liquid at the given temperature, g/cm^3

The theoretical density of PP/EPR/CB composites can be calculated as follow

$$\text{Theoretical density} = (\rho_{PP}V_{PP}) + (\rho_{EPR}V_{EPR}) + (\rho_{CB}V_{CB}) \quad (5.2)$$

Where

ρ_{PP} = density of polypropylene, g/cm^3

ρ_{EPR} = density of ethylene propylene rubber, g/cm^3

ρ_{CB} = density of carbon black, g/cm^3

V_{PP} = polypropylene volume fraction

V_{EPR} = ethylene propylene rubber volume fraction

V_{CB} = carbon black volume fraction

The densities of all PP/EPR/CB composites were observed to increase systematically with increasing CB contents following a rule of mixture and the values are compared in Table 5.1. From the table, the measured densities are in good agreement with the theoretical values in all PP/EPR/CB composites with an error of less than 1% (i.e. the densities of PP/CB composites at CB content ranging from 0 to 30 wt% comparing with their theoretical densities are shown in Figure 5.1). From the result, it can conclude that these polymer blends contained negligible void in the obtained specimens.

5.2 Differential Scanning Calorimetry (DSC) of PP, EPR, and PP/EPR Blends

Figure 5.2 shows DSC thermograms of PP, EPR, and PP/EPR blends at blend ratios ranging from 100/0 to 0/100 wt/wt and the important parameters are also summarized in Table 5. According to the results, both PP and EPR show positions of the endothermic melting peaks at 168 and 146 $^{\circ}$C, respectively. For the PP/EPR blends, the melting temperature of the EPR phase was observed to systematically shift to higher temperature with increasing PP content. However, the melting temperature of the PP domain was found to slightly shift to lower temperature with increasing PP content. This observation suggests some interaction between the PP and EPR phases, which is attributed to the partial miscibility between molecules of PP and EPR. Similar behavior was also observed by Qin et al. in the case of PP

blended with mLLDPE [38]. In principle, the blends that exhibit partially miscible or immiscible characteristics are appropriate for making filled composites with minimal filler concentration by utilizing the "double percolation" approach [39, 40]. Furthermore, the heat of fusion of the PP was determined to be 91 J/g and that of the EPR was 27 J/g. This clearly suggests the more crystalline nature of the PP compared to the EPR. In addition, the substantial amount of the heat of fusion value of the neat EPR polymer also implies that this copolymer is not a totally random or alternating type but contains some order structure or crystalline domains in it. The heat of fusion values of the PP/EPR blends were also found to decrease with increasing EPR content. This phenomenon is attributed to the total crystallinity of the blended matrix to be decreased from the added less crystalline EPR fraction.

5.3 Dynamic Mechanical Analysis (DMA) of PP/EPR Blends

Storage modulus (E′), loss modulus (E″) and loss tangent (Tanδ) obtained from DMA tests were utilized to characterize PP, EPR and PP/EPR blend at a weight ratio of 50/50 as shown in Figure 5.3-5.5. The storage moduli of PP, EPR and PP/EPR blend at a mass ratio of 50/50 wt% are shown in Figure 5.3. According to the thermograms, storage modulus at room temperature of PP was determined to be 1.84 GPa while that of ERP and PP/EPR blend ratio of 50/50 were about 1.03 GPa and 1.47 GPa, respectively. The storage modulus at room temperature of the PP/EPR blend was observed to decrease with the presence of EPR in the blend due to the fact that EPR is softer than PP. Furthermore, they exhibited two-step changes corresponding to the positions of glass transition temperature (T_gs) of the PP and EPR phases. From the figure, the positions of T_gs of both PP and EPR phases in the blend were also found to slightly shift towards each other. The above characteristics suggest partially miscible nature of this PP/EPR blend. Furthermore, the greater change in slope of the storage modulus curve vs. temperature of EPR compared to that of PP is one parameter indicating better thermal stability of the PP compared to the EPR and their blend.

Glass transition temperatures of PP, EPR and PP/EPR blends at a weight ratio of 50/50 were determined from the DMA thermograms based on the peaks of loss modulus. In principle, a miscible polymer blend usually exhibits single glass transition temperature (T_g). Whereas in a partially miscible blend, two T_gs of each starting polymer component will be observed and the T_g of each component usually shifts towards each other as a function of blend composition. In the case of immiscible blend, two T_g values can be detected which are the T_g values of the two starting polymers [41, 42]. Figure 5.4 illustrates the loss modulus curves of PP, EPR and PP/EPR blends. From the peak position in each curve, the thermograms of the neat PP clearly revealed a single T_g at 4°C while that of EPR showed a single T_g at -21°C. Additionally, from this figure, the PP and EPR mixture clearly gave two T_gs which shifts towards each other since the two materials are partially immiscible in nature as mentioned earlier. In addition, Figure 5.5 exhibits α-relaxation peaks of the loss tangent (tan δ) of the PP, EPR and their blend. From this figure, it was found that the peak maxima of the loss tangent showed the same characteristics as observed in the loss modulus peaks for PP, EPR and the partially miscible PP/EPR blend though at relatively higher values of the corresponding peak positions.

5.4 Rheological Properties of Neat PP and EPR

Complex viscosities of PP and EPR as a function of shear rate measured at 210°Cwere shown in Figure 5.5. From this figure, it was observed that melt viscosities of PP and EPR decreased with increased shear rate, suggesting non-Newtonian behavior of a shear thinning type of these polymers. As can be seen, the viscosity of PP is higher than that of EPR over all the frequency ranges.

According to Paul and Barlow relation [18], Equation 5.3, the ratio of melt viscosity of PP and EPR is shown as follows:

$$\frac{\phi_1}{\phi_2} = \frac{\eta_1}{\eta_2} \qquad (5.3)$$

where η_i and ϕ_i are the melt viscosity and volume fraction of polymers, respectively.

In general, the viscosity ratios or the blending ratios of two polymers (to generate co-continuous phase) depend on the shear rate during operation. Different processing methods (i.e. compression, extrusion and injection) could lead to different shear rates. Therefore, the volume ratios of blending between two polymers to form co-continuous phase are different. For the compression methods, the shear rates of processing are in the range of 1-10 s^{-1}, while those of extrusion methods are in the range of 10-100 s^{-1} [43].

In our study, at low shear rate (2.9 s^{-1}), the melt viscosity of PP and EPR is 1391 Pa·s and 535.2 Pa·s, respectively. The ratio of melt viscosity of PP and EPR is 2.60. For high shear (34.1 s^{-1}), the melt viscosity of PP and EPR is 295.1 Pa·s and 183.2 Pa·s, respectively. The ratio of melt viscosity of PP and EPR is 1.61. From the equations of Paul and Barlow will be the ratio of the volume of PP/ EPR to cause a co-continuity, which was observed 72/28 (ca. 2.60) to 62/38 (ca. 1.61).

5.5 Morphology of PP/EPR Blends

To investigate the phase morphology of the PP/EPR blends, the sample surfaces were coated with a thin layer of gold before taking the micrographs by scanning electron microscope (SEM). Figures 5.7a-5.7f show the freeze-fracture surface of CB-filled PP/EPR blends at the weight ratios ranging from 100/0 to 50/50. The discontinuous EPR domains in PP matrix were observed in the PP/EPR blends with EPR of less than 20% by weight. The EPR domain shape had been changing from small oval shape to more elongated shape with increasing fraction of EPR as shown in Figure 5.7a-5.7c. Moreover, For the CB filled PP/EPR blends of greater than 30% by weight (Figure 5.7d-5.7f); the increase of EPR resulted in the formation of EPR continuous structure as seen in the figure. In this EPR contents of 30-50% by weight, both PP domains and EPR domains tended to form continuous structure in the continuous PP matrix, which is known as co-continuous phase structure. Consequently, the co-continuous phase can be obtained and can be used as a platform to produce a "double percolation" morphology when CB is added. This double percolation structure is one of the most promising methods to reduce the

percolation threshold and to enhance the composite conductivity at lower loading of conductive filler [6-13, 39, 40].

5.6 Effects of Blend Ratios on Electrical Properties of CB-Filled PP/EPR Blends

Figure 5.8 depicts a relationship between volume resistivity and EPR content of CB-filled PP/EPR blends at a fixed CB content of 5 wt%. The corresponding numerical results are summarized in Table 5.4. In each single polymer (i.e. 100% PP or 100% EPR), although both polymers contained 5 wt% CB, the materials are clearly insulators as the volume resistivity of both polymers are higher than 10^{11} Ω.cm [22]. For the PP/EPR blends at weight ratios ranging from 80/20 to 30/70, the CB-filled PP/EPR blends were found to be evidently more conductive and their volume resistivity values exhibited a minimum value of 5.0×10^{4} Ω.cm at the PP/EPR blend ratio of 50/50 indicating the highest conductivity as seen in Figure 5.8. Increasing the EPR fraction greater than 50 wt%, the volume resistivity tended to increase again to higher values due to the dilution of the constant amount of CB localized in the EPR phase. It is likely that a double percolation effect might take place in the blends containing EPR of about 50 wt% or in this vicinity when the total CB content is 5 wt% in the PP/EPR blends. Then above the EPR content of 50 wt%, the volume resistivity starts to increase with the EPR content. This result is in good agreement with the work reported by Gubbels and coworkers in the PE/PS blends filled with CB [44] and Sumita and coworkers in the PMMA/HDPE blends filled with CB [34]. That is the increasing amount of the minor phase polymer of partially miscible or immiscible blends, which contains conductive filler can show double percolative behavior. The volume resistivity of the blends will exhibit a minimum value at the point around the co-continuous phase morphology when the amount of the conductive filler is fixed.

5.7 Electrical properties of PP/EPR/CB composites

Figure 5.9 shows the volume resistivity of CB-filled PP and PP/EPR blends. All the composites exhibit typical characteristics of percolation phenomenon. At low CB loadings, a little change in volume resistivity can be observed because the distances

between CB particles are large enough. The increase of CB content makes particles more crowded, leading to the slow decrease of volume resistivity. The volume resistivity decreases dramatically, in the vicinity of the percolation threshold, where the transition from insulating to conductive materials occurs. This indicates CB particles came into contact with each other or closed up enough to allow the electron hop by tunneling, thus forming continuous conducting paths or network. Once the percolative network was formed, additional CB loading could not significantly reduce the volume resistivity because of the formation of conducting paths [32, 45]. The percolation threshold of CB-filled polymers, in our case, was determined at the volume fraction of CB that the compounds change from insulative (> 10^{11} Ω cm) to conductive (< 10^4 Ω cm) [22].

In CB added PP/EPR blend systems, the percolation threshold depend strongly on the phase morphology and the distribution of CB in the polymer blends. Figure 5.9 shows the volume resistivity curves of PP/EPR blends at the weight ratios ranging from 100/0 to 50/50 with CB as conductive filler ranging from 0 to 30 wt%. It was observed that the percolation threshold of CB-filled PP is about 6-13 wt% CB. The percolation regions of the PP/EPR-based composites were lower than those of PP-based composites and they were shifted to the left. For example, PP/EPR mixtures at 20 to 50 wt% EPR with 10 wt% CB provided a volume resistivity of about 10^3 Ω·cm, which was a much lower than that of the PP/CB systems. The percolation threshold of PP/EPR mixtures at 20 to 50 wt% EPR was observed at about 2-6 wt% CB, where the volume resistivity changed by 11 orders of magnitude. To achieve the volume resistivity of less than 10^4 Ω·cm, the CB content in the blend can be reduced at least 50% compared to the composite using neat PP as a matrix.

As shown in Figure 5.9, an interesting phenomenon was found in the electrical properties of CB-filled PP/EPR blend ratio of 90/10. The percolation threshold is about 6-13 wt% CB, which is substantially higher than that of the other PP/EPR blends. For the PP/EPR blend ratio of 90/10, PP forms continuous phase and minor EPR fraction forms dispersed phase. If the CB selectively disperses in the PP phase, the CB content would reach the percolation threshold of PP and leads to

conductive composite. Therefore, the higher percolation threshold of composite suggests that CB can be preferentially presented in the EPR phase. According to the Figure 5.9, the volume resistivity values measured from these composites are sensitive to blend compositions. Increasing the EPR content in the blend will lead to the decrease in volume resistivity. Additionally, the CB content where percolation commences in the polymer blend composite is lower than that in the single polymer composite. This phenomenon is attributed to the double percolation arising from the heterogeneous distribution of the conductive filler in one phase of the blended matrix [45-49].

Figure 5.10 shows the surface resistivity curves of PP/EPR blends at the weight ratios ranging from 100/0 to 50/50 with CB as conductive filler ranging from 0 to 30 wt%. From this figure, it was found that the percolation threshold of the surface resistivity showed the same characteristics as observed in the volume resistivity for all PP/EPR/CB composites. Furthermore, to achieve the surface resistivity of less than 10^6 Ω/square, the CB content in the blend can be reduced compared to the volume resistivity measured for usage as conductive material.

5.8 The Selective Distribution of CB Particles into PP/EPR Blends

Recently, one promising method to reduce the amount of conductive fillers in composites is to use immiscible or partially miscible polymer blends. The selective localization of CB in one of the phases of the polymer blend is a very efficient strategy to decrease the CB percolation threshold. The phenomenon is known as a double percolation behavior [45-49]. The selective localization of CB depends on surface tension, viscosity, degree of crystallinity of components and process of polymer blends [25, 28] as follows:

- CB particles selectively locate in one of two polymer phases where a lower interfacial tension between polymer and CB in obtained that is predicted by Young's equation.

- The percolation threshold of semi-crystalline polymer are lower than amorphous polymer due to CB are unable to penetrate the crystalline regions, they

are preferentially isolated entirely in the amorphous region. Thus, CB particles prefer to accumulate in the amorphous than semi-crystalline polymer.

- When the polymer components exhibit different melt viscosities, CB is found to accumulate in the polymer component with the lower viscosity during processing.

For PP/EPR blend, CB are expected to be selectively located in EPR phase because 1) the interfacial tension between EPR and CB (γ_{EPR-CB} = 1.9 mJ/m^2) is lower than PP and CB (γ_{PP-CB} = 1.9 mJ/m^2) [13, 50]. 2) PP has more crystallinity than EPR therefore the penetration of CB into PP phase tends to be more difficult than EPR. Finally, the viscosity of EPR used is lower than PP. From those three reasons, it is very likely that the CB particles should be presented in the ERP phase than in the PP phase. To elucidate the selective localization of the CB in the PP/EPR blends, the scanning electron microscope of freeze-fracture surface of CB-filled PP/EPR blends has been performed as shown in Figure 5.11a-5.11c.

Figure 5.11a shows CB particles which were used as conductive filler in PP, EPR, and PP/EPR blends. The micrographs revealed relatively good distribution of CB in both PP and EPR homopolymer with the observed aggregate size to be in the range of 0.3-1 μm. Note that CB aggregates are visualized as bright aggregate in the micrograph even though the whole surface were coated with a thin layer of gold. Additionally, the different distribution of CB in PP domains as well as CB in EPR domains in PP/EPR blend at a fixed blend ratio of 70/30 with 5 wt% CB can be evidently observed in Figure 5.11c. This selective distribution of CB in the EPR phase is attributed to its lower interfacial free energy, crystallinity, and viscosity compared to PP phase as discussed above.

5.9 Morphology of CB-Filled PP/EPR Blends

Figure 5.12a-5.12f show the freeze-fracture surface of CB-filled PP/EPR blends at the weight ratios ranging from 100/0 to 50/50 with CB as conductive at a fixed CB content of 5 wt%. The result from microscope illustrated the preferential localization of CB in the EPR phase. The discrete domains of selective distribution CB in the EPR

phase into PP matrix were observed in PP/EPR blends of 100/0, 90/10, 80/20 and 70/30 with domain shape changing from more spherical shape to oval or more elongated shape with increasing fraction of EPR as shown in Figure 5.12a-5.12d. Furthermore, For the CB filled PP/EPR blends of 60/40 (Figure 5.12e) and 50/50 (Figure 5.12f), the increase in the EPR at about this high contents resulted in the formation of EPR continuous structure as seen in the figure. It is clearly seen that without CB, the co-continuous structure will occur at the EPR content about 30 wt% in PP whereas with the presence of CB (5 wt%), the co-continuous structure in the PP/EPR blend was found to shift to higher EPR content i.e. 40 wt%. This result was in good agreement with the work reported by Breuer and coworkers in the HIPS/LLDPE blends filled with CB [51]. At this point, both PP domains as well as CB particles in the EPR domains formed continuous structures, which are known as a double percolative structures that can reduce the percolation threshold of the CB used.

According to Paul and Barlow relation [18], Equation (5.3), which gives a general trend for co-continuity formation based on blend components relative viscosities, introducing CB into EPR phase increased the EPR phase viscosity and consequently increased the volume fraction required to achieve co-continuity. Existence of CB in one phase of blend matrix is postulated to increase the friction between the major phase and dispersed phase. Such increase of friction could lead to some deformations producing elongated dispersed morphologies [51].

5.10 Effect of Processing Sequence on the Electrical Properties

In this work, the effect of different processing sequence on the electrical properties was investigated. In addition to the simultaneously melt-mixtures of PP+EPR+CB, (PP + CB)/EPR, (EPR + CB)/PP and (PP + EPR)/CB blends were the compounds prepared by pre-melt blending CB with PP (or EPR) followed by the addition of EPR (or PP) or blending PP with EPR followed by the addition of CB. Table 5.5 shows the volume resistivity of 5-10 wt% of CB-filled PP/EPR at a blend ratio of 70/30 with different processing sequence. For the 5 wt% CB-filled PP/EPR blend ratio of 70/30, the volume resistivity of the simultaneously melt-blended, (PP + EPR)/CB

and the (EPR+CB)/PP samples is about the same (4.2-5.7×10^5 Ω cm). While the volume resistivity of the (PP + CB)/EPR sample is higher (i.e. 1.6×10^6 Ω cm). For the (EPR + CB)/PP composite, CB preferentially localizes in the EPR phase, as in the simultaneous melt-blended and (PP + EPR)/CB samples. The migration of CB from the EPR phase to PP rarely occurs because of the better affinity between EPR and CB than PP and CB. However, the addition of EPR into PP/CB caused the migration of CB from the PP domains to the EPR domains, reducing the CB concentration in the continuous PP matrix, thus resulted in an increase in the volume resistivity of the specimen. The trend of CB to preferentially migrate from PP to EPR phases is probably due to the lower melt viscosity of ERP at the processing temperature and the lower interfacial surface tension of EPR and CB compared to PP and CB. Similar behavior was also reported in PP/PS/CB composite by Al-Saleh et al. [10]. For the 10 wt% CB-filled PP/EPR at a blend ratio of 70/30, the processing sequence had no significant effect on the volume resistivity of conductive polypropylene composites. This might because the CB concentration already exceeds the percolation threshold.

5.11 Tensile Properties of CB-Filled PP/EPR Blends

Figures 5.13-5.15 show tensile properties of PP/EPR blends at weight ratios ranging from 100/0 to 50/50 with CB as conductive filler ranging from 0 to 20 wt%. Tensile moduli of PP/EPR/CB composites as a function of CB and EPR content were plotted in Figure 5.13. As the CB content increased, an increase in the modulus value or the brittleness was observed. The tensile modulus increased with increasing CB content as expected since CB is stiffer than PP and EPR. Similar enhancement in stiffness was observed for other polymers reinforced by CB [52, 53]. Additionally, the tensile modulus of PP/EPR/CB composites expectedly decreased with increasing EPR fraction due to the introduction of the softer elastomeric content into the blends. Similar behavior was also observed by Farshidfar et al. in the case of HDPE blended with EPDM having CB as a conductive filler [11].

Tensile strength values of PP/EPR/CB composites are shown in Figure 5.14. The tensile strength of the composites at PP/EPR blend ratios of 100/0, 90/10 and

80/20 was observed to slightly decrease with increasing CB content. The addition of 5 wt% of CB at PP/EPR blending ratios of 70/30, 60/40 and 50/50 led to the increase of the tensile strength. The tensile strength values were also found to slightly decrease with greater CB contents of 5-20 wt% used in the experiment. As shown in this figure, the tensile strength values of the PP/EPR/CB composites were found to decreases with increasing CB content. It is postulated that the aggregation and agglomeration may present in the CB thus cause some defects in the composites resulting in lowering of the tensile strength values. These observed phenomena are often observed in CB-filled systems e.g. CB-PP [20], and CB-EVA [54]. Moreover, the tensile strength for PP/EPR/CB composites was found to decrease with increasing EPR content as well. Despite the reduced tensile strength, all the tensile strength values of our PP/EPR/CB composites were still much higher than the target value of tensile strength of commercial conductive PP i.e. > 21 MPa [55].

Elongation at break of PP/EPR/CB composites is shown in Figure 5.15. It is clearly seen from the figure that an increase in the CB particles tended to lower the elongation at break of the resulting composites. On the other hand, we can see that the previously mentioned problem can be solved by an addition of the EPR in PP. In this figure, an increase of EPR content can substantially increase the elongation at break of the composite samples. It could be noticed that the elongation at break of the neat PP was lower than that of PP/EPR blend comparing at the same CB loading because EPR exhibits the elastic properties of rubber material, which is generally easier to draw. Normally, the rubber material has lower modulus but higher elongation that is opposite to brittle material. The addition of the CB into PP/EPR blends reduced the elongation at break of the composites, which indicated that the toughness of composites was reduced. In addition, the values of elongation at break for the PP/EPR/CB composites were slightly higher than PP/CB composites due to the ductile effect of the EPR.

5.12 Notched Izod Impact Strength of CB-Filled PP/EPR Blends

Figures 5.16 shows impact strength values of PP/EPR blends at varied weight ratios ranging from 80/20 to 60/40 with CB as conductive filler ranging from 0 to 20 wt%. As the CB content increased, the impact strength values were observed to slightly increase. This might suggest the substantial interfacial bonding between the CB and the polymer matrix which might provide the additional energy absorption processes such as debonding mechanism thus the observed slight increase in the impact strength values [56]. In addition, the incorporation of the more amount of the EPR fraction in the blends expectedly increased the impact strength values of the blends at all ranges of the CB loadings as a result of an increase in the soft rubbery component in the compounds. Similar behavior was also observed by Lee et al. in the case of PP blended with POE having SiO_2 as a filler [57].

5.13 Melt Flow Index (MFI) of PP/EPR and CB-Filled PP/EPR Blends

In this measurement, MFI values of all PP/EPR blends and PP/EPR/CB composites measured at 230°C under an applied load of 2.16 kg are shown in Figure 5.17. From this figure, it was found that the MFI values of the PP/EPR blending ratios of 80/20, 70/30 and 60/40 were 2.5, 2.9 and 3.3 g/10min, respectively. Additionally, comparing at the same CB loading, it were found that MFI values of the blends increased systematically with increasing the mass fraction of EPR due to the fact that EPR possesses higher MFI value or higher flowability than that of PP. The MFI values of PP/EPR/CB composites were slightly decreased with CB as conductive filler loading ranging from 0 to 20 wt%. On the other hand, the MFI values for PP/EPR/CB composites were systematically increased with increasing EPR content and the value was raised by 20% when the EPR was increased from 20% to 40%. Those MFI values of all PP/EPR blends and PP/EPR/CB composites are also summarized in Table 5.6.

5.14 Thermogravimetric Analysis (TGA) of CB-Filled PP/EPR Blend

TGA thermograms under nitrogen of PP/EPR blend at a fixed blend ratio of 70/30 with CB as conductive filler ranging from 0 to 30 wt% are shown in Figure 5.18. The corresponding numerical results are summarized in Table 5.7. The temperatures corresponding to 5 % weight loss ($T_{5wt\%}$) are essential to evaluate the decomposition of PP/EPR/CB composites on onset stage. $T_{5wt\%}$ was found to increase with the increase of CB content as seen in the Figure 5.19. It is apparent that thermal decomposition temperature at $T_{5wt\%}$ for PP/EPR/CB composites shifted significantly to a higher temperature range than that of the neat PP/EPR blend, which indicated an improvement of thermal stability of the polymeric matrix due to the presence of the CB filler. Therefore, PP/EPR blend ratio of 70/30 with 30 wt% CB (maximum content in this system) exhibited the highest $T_{5wt\%}$ (455 ^{o}C), which was shifted approximately 25 ^{o}C towards high temperature compared to that of the neat PP/EPR blend. This substantial enhancement in the thermal properties of the CB-filler PP/EPR blend is likely due to the barrier effect of CB in the composites [58]. The degradation temperature tends to increase with increasing the amount of the conductive filler in the polymer matrix had been observed in the systems of CB particles filled-PP composites [59].

The relationship between CB contents and residual char of the PP/EPR/CB composites is also illustrated in Figure 5.19 and the corresponding numerical values listed in Table 5.7. CB filler exhibits very high thermal stability thus does not experience any significant weight loss (0.4 wt%) within the temperature range of 30-800 ^{o}C under the TGA investigation [60]. When the temperature was raised to 800 ^{o}C, mainly the PP/EPR fraction was decomposed thermally and formed char. Therefore, the amounts of char residue in this case can be approximated to correspond directly to the content of the CB filler plus char residue of the PP/EPR fraction.

Figure 5.20 shows the degradation temperature and residual char of PP/EPR/CB composites at a fixed CB content of 10 wt% with PP/EPR blends at weight ratios ranging from 100/0 to 50/50 under nitrogen. As seen in this figure, the thermal decomposition behavior of the composites was almost the same. Consequently, it

can be concluded that the varied blend ratios of PP and EPR showed no influence on their thermal decomposition temperature and char residue. This is due to their analogy in chemical constituents of the PP and the EPR, thus reflecting the same thermal behaviors. The corresponding numerical results of all PP/EPR/CB composites are also summarized in Table 5.8.
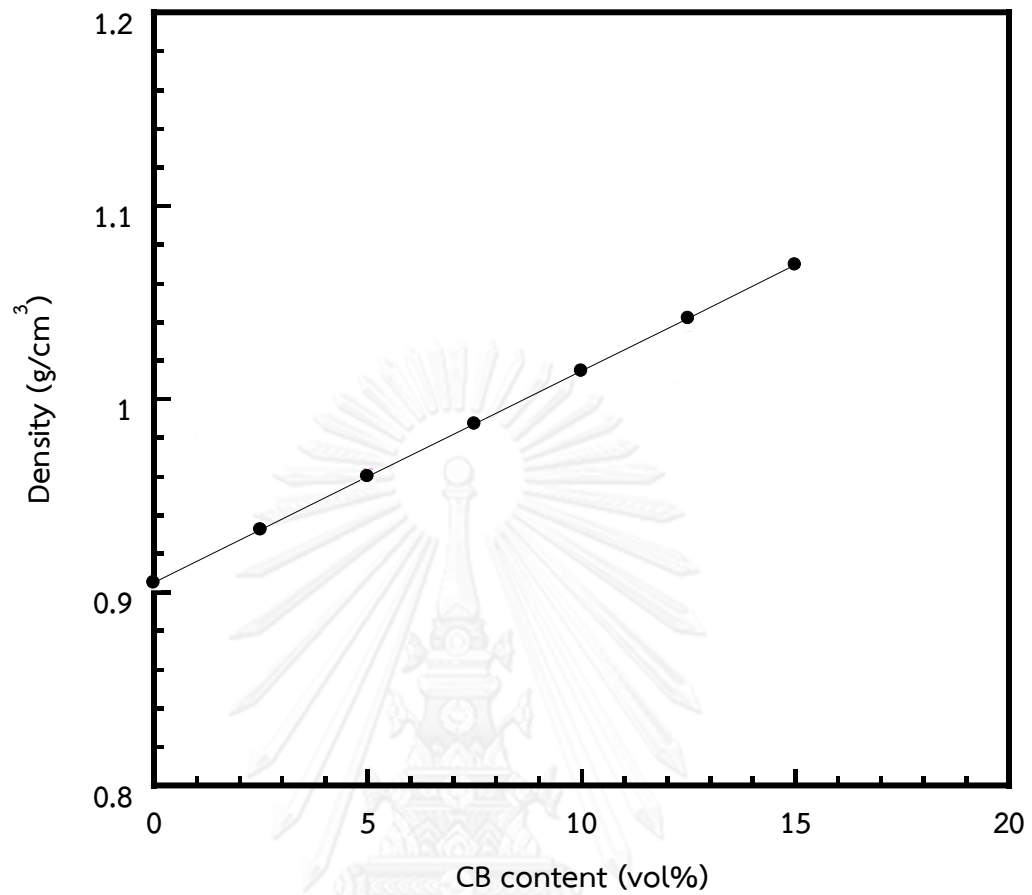
Figure 5. 1: Density versus blend ratios of PP/CB composites: (▲) actual density and
(●) theoretical density.

Table 5. 1: Actual and theoretical densities of all CB-filled PP/EPR blends at various blend ratios.

| CB content (wt%)	Theoretical density (g/cm^3)			Actual density (g/cm^3)		
	100/0	90/10	80/20	100/0	90/10	80/20
0	0.905	0.904	0.902	0.905	0.902	0.900
5	0.932	0.931	0.930	0.930	0.928	0.927
10	0.960	0.958	0.957	0.961	0.957	0.955
15	0.987	0.986	0.985	0.985	0.983	0.980
20	1.015	1.013	1.012	1.014	1.010	1.009
25	1.042	1.041	1.039	1.039	1.034	1.035
30	1.069	1.068	1.067	1.068	1.061	1.064
	70/30	60/40	50/50	70/30	60/40	50/50
0	0.901	0.899	0.898	0.900	0.899	0.898
5	0.928	0.927	0.926	0.928	0.928	0.925
10	0.956	0.954	0.953	0.954	0.950	0.955
15	0.983	0.982	0.981	0.980	0.981	0.978
20	1.011	1.009	1.008	1.013	1.006	1.002
25	1.038	1.037	1.036	1.035	1.035	1.031
30	1.066	1.064	1.063	1.064	1.061	1.060
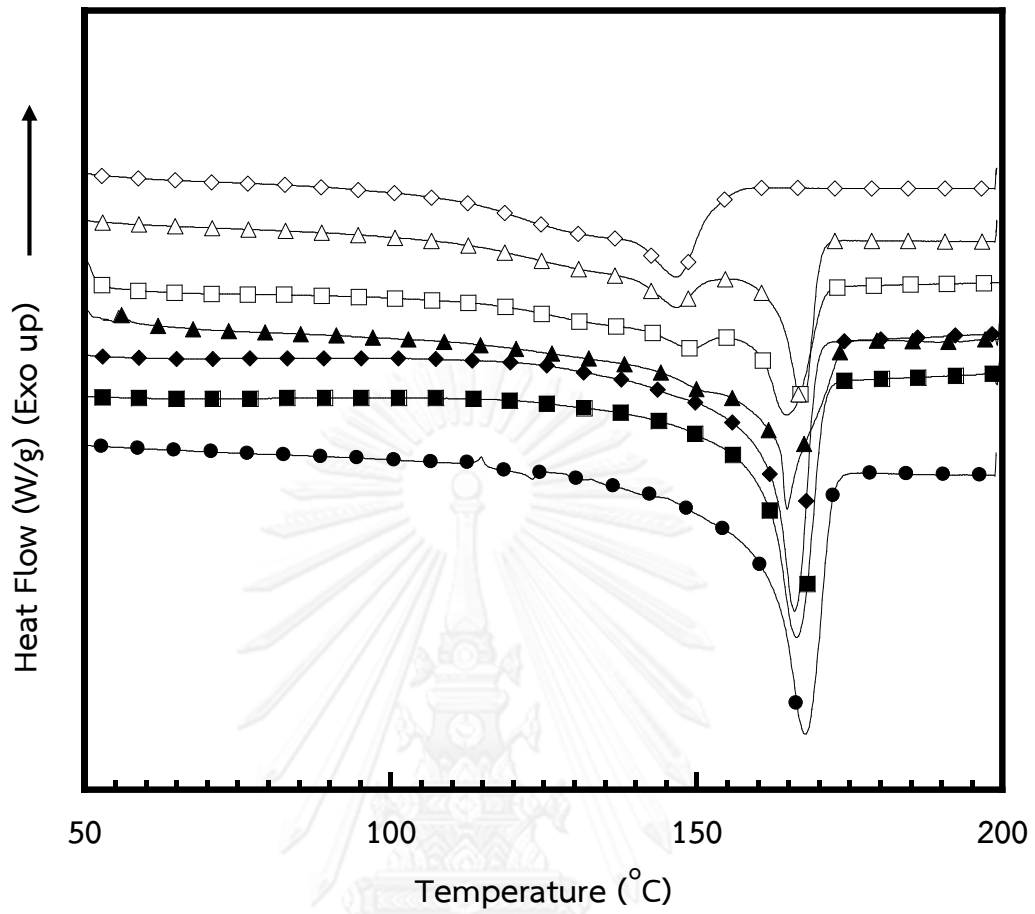
Figure 5. 2: Differential scanning calorimetry (DSC) thermograms of PP/EPR blends at various blend ratios: (●) 100/0, (■) 90/10, (◆) 80/20, (▲) 70/30, (□) 60/40, (△) 50/50 and (◇) 0/100.

Table 5. 2: Melting temperature (T_m) and melting enthalpy (ΔH_m) of PP/EPR blends at various blend ratios.

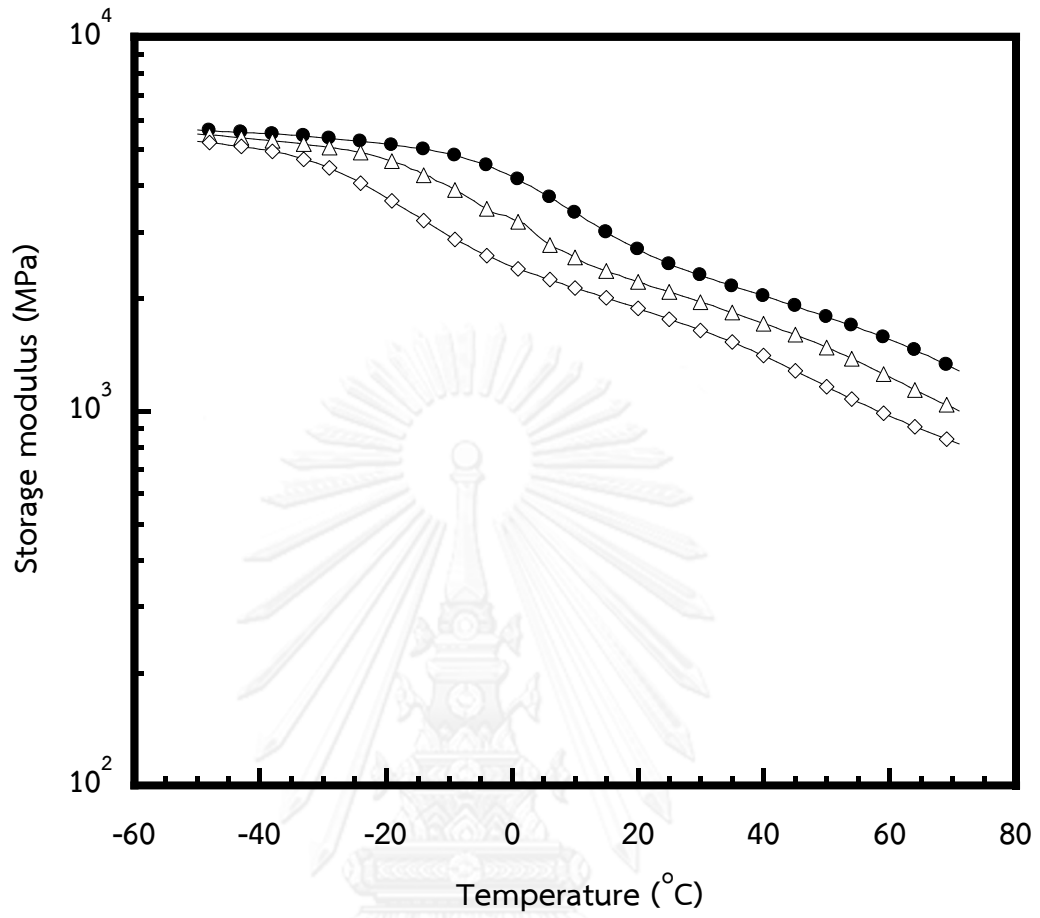| PP/EPR blend ratio	T_m (°C)		ΔH_m
	T_{m1}	T_{m2}	(J/g)
100/0	-	168	91
90/10	**	166	84
80/20	**	165	76
70/30	152	163	59
60/40	150	165	57
50/50	148	166	56
0/100	146	-	27

Note: (**) Undetectable

Figure 5. 3: Storage modulus versus temperature (°C) of PP/EPR blends at various blend ratios: (●) 100/0, (△) 50/50 and (◇) 0/100.
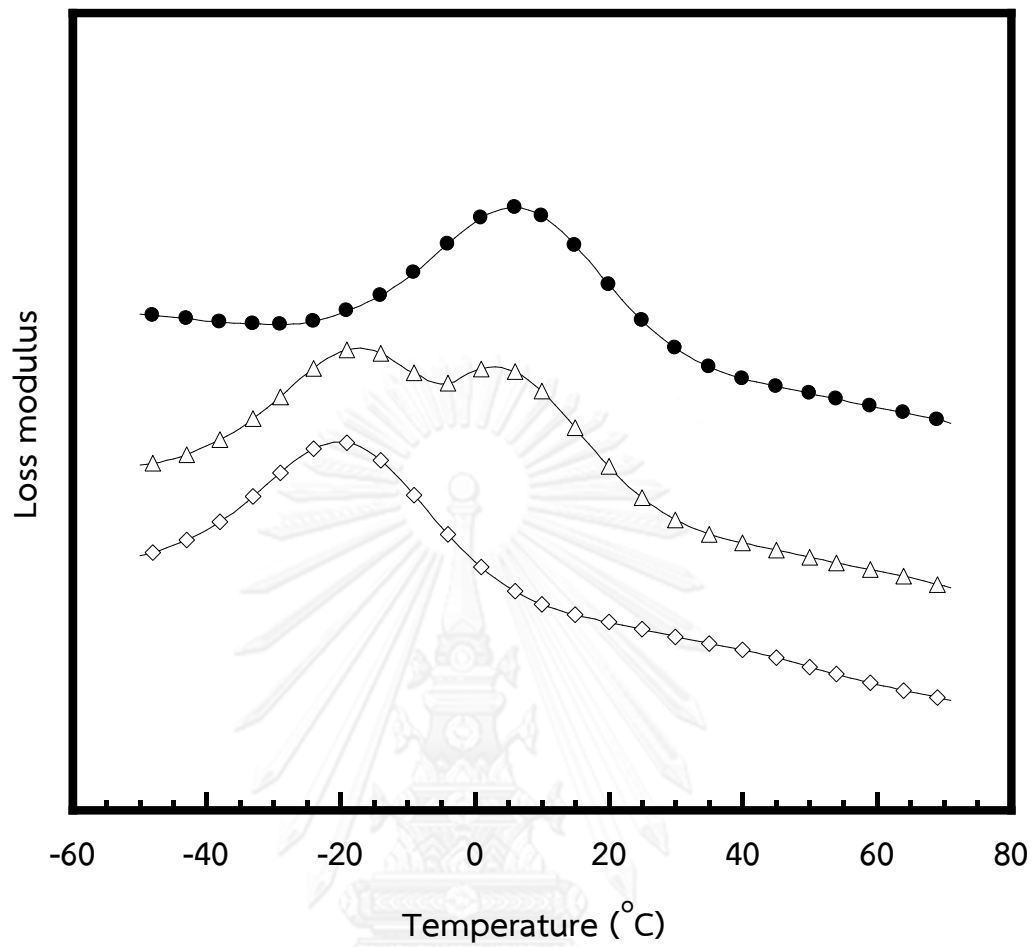
Figure 5. 4: Loss modulus versus temperature (^{o}C) of PP/EPR blends at various blend ratios: (●) 100/0, (△) 50/50 and (◇) 0/100.
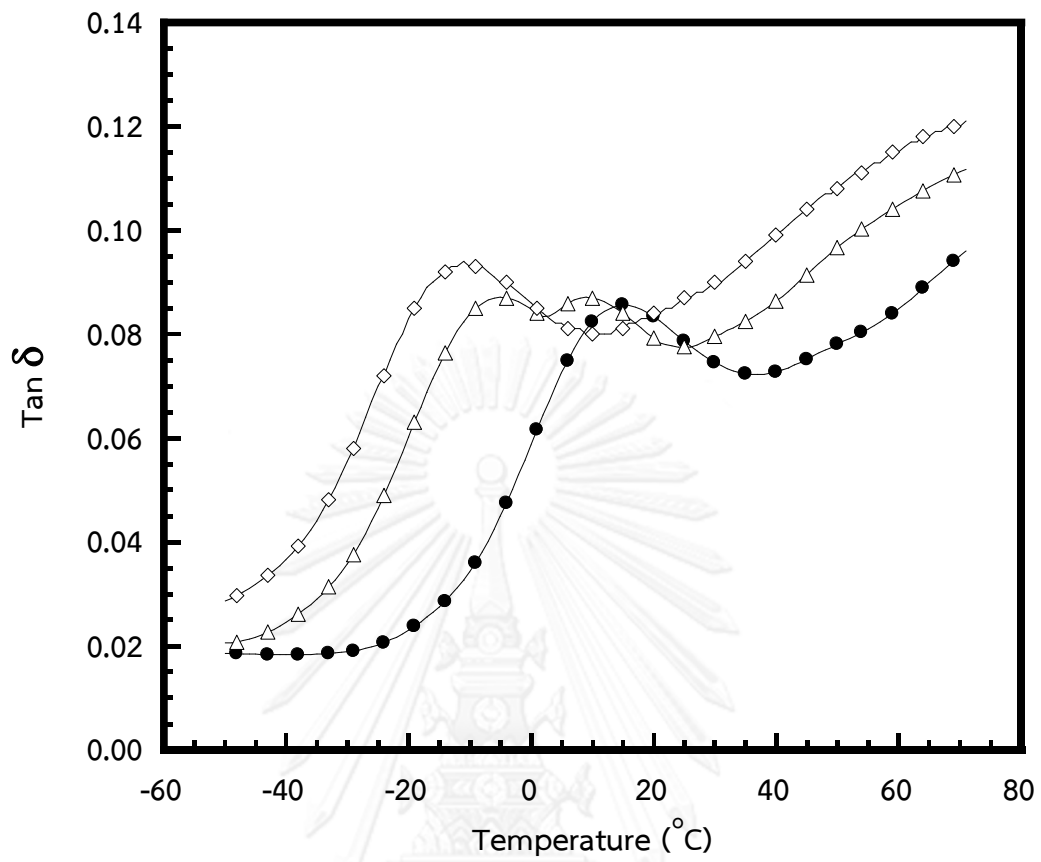
Figure 5. 5: Loss tangent versus temperature ($^{\circ}$C) of PP/EPR blends at various blend ratios: (●) 100/0, (△) 50/50 and (◇) 0/100.

Table 5. 3: Glass transition temperatures of PP/EPR blends at various blend ratios from loss modulus curves.

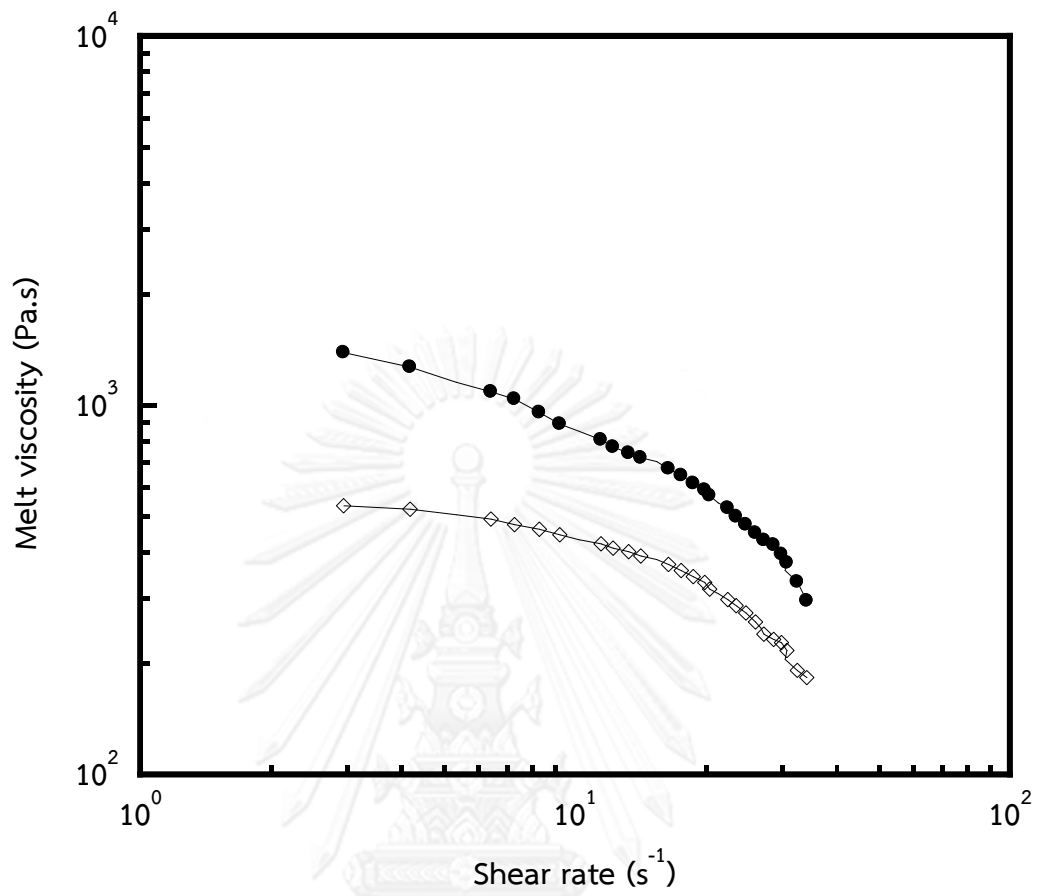| PP/EPR blend ratio	T_g (°C)	
	T_{g1}	T_{g2}
100/0	-	4
50/50	-17	2
0/100	-21	-

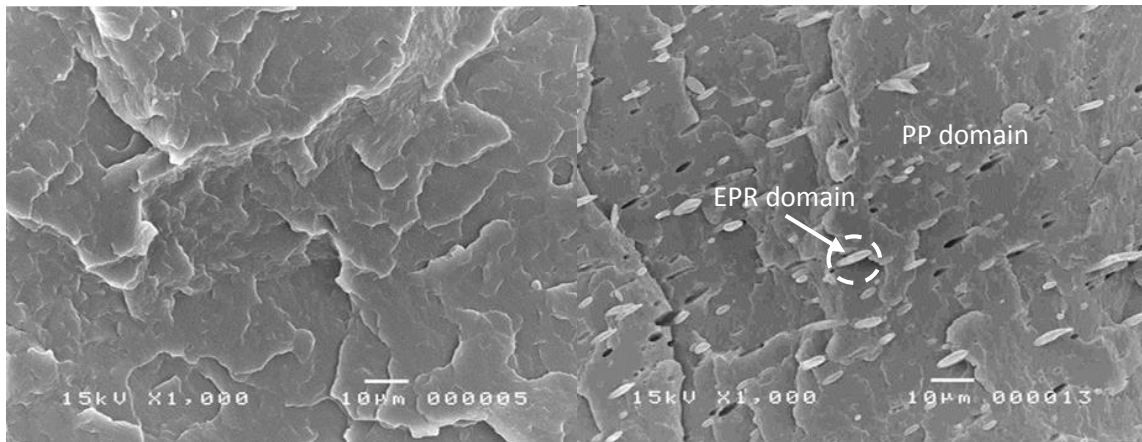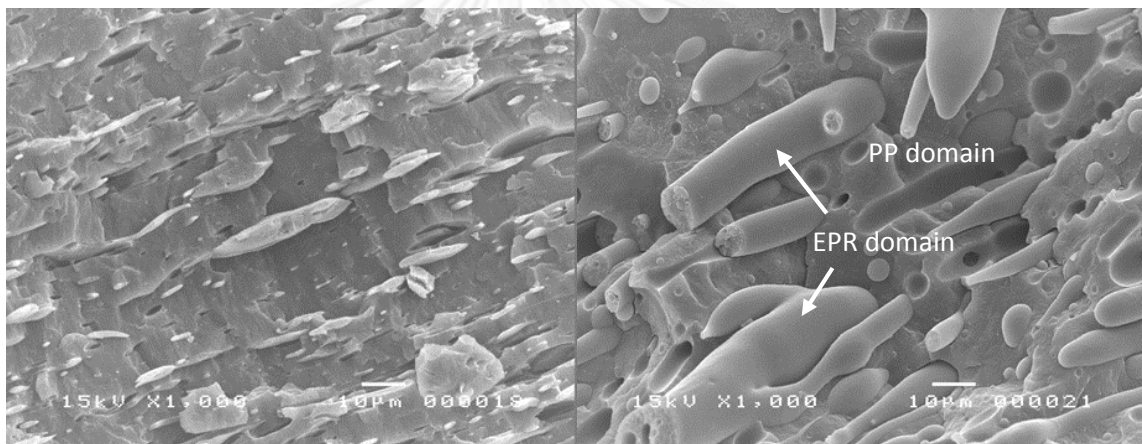**Figure 5. 6:** Shear rate dependence of melt viscosity at 200 °C: (●) PP and (◇) EPR.
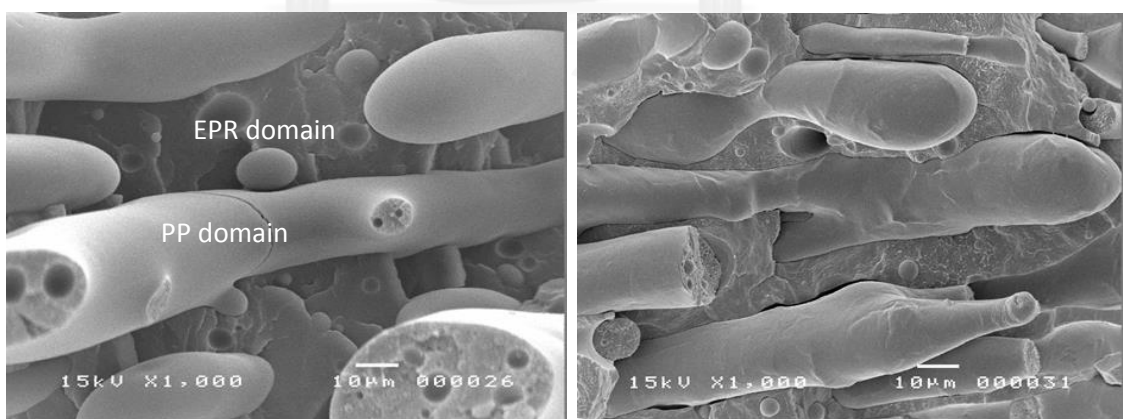
Figure 5. 7: SEM micrographs of freeze-fracture surface of PP/EPR blend at various blend ratios: (a) 100/0 (b) 90/10 (c) 80/20 (d) 70/30 (e) 60/40 and (f) 50/50.

Figure 5. 8: Volume resistivity of 5 wt% CB-filled PP/EPR blends at various blend ratios.

Table 5. 4: Volume resistivity of 5 wt% CB-filled PP/EPR blends at various blend ratio.

PP/EPR blend ratio	Volume Resistivity (Ω·cm)	Log Volume resistivity (Ω·cm)
100/0	1.2×10^{15}	15.1
90/10	1.0×10^{15}	15.0
80/20	3.9×10^{6}	6.6
70/30	3.9×10^{5}	5.6
60/40	7.9×10^{4}	4.9
50/50	5.0×10^{4}	4.7
40/60	2.5×10^{5}	5.4
30/70	6.3×10^{6}	6.8
0/100	1.2×10^{15}	15.1

Figure 5. 9: Volume resistivity of CB-filled PP and PP/EPR blends at various blend ratios: (●) 100/0, (■) 90/10, (◆) 80/20, (▲) 70/30, (□) 60/40 and (△) 50/50.

Figure 5. 10: Surface resistivity of CB-filled PP and PP/EPR blends at various blend ratios: (●) 100/0, (■) 90/10, (◆) 80/20, (▲) 70/30, (□) 60/40 and (△) 50/50.

(a)   (b)

(c)

Figure 5. 11: SEM micrographs of freeze-fracture surface of CB-filled PP/EPR blends: (a) pure CB (b) 5 wt% CB-filled PP and (c) 5 wt% CB-filled PP/ERP blend ratio (70/30).
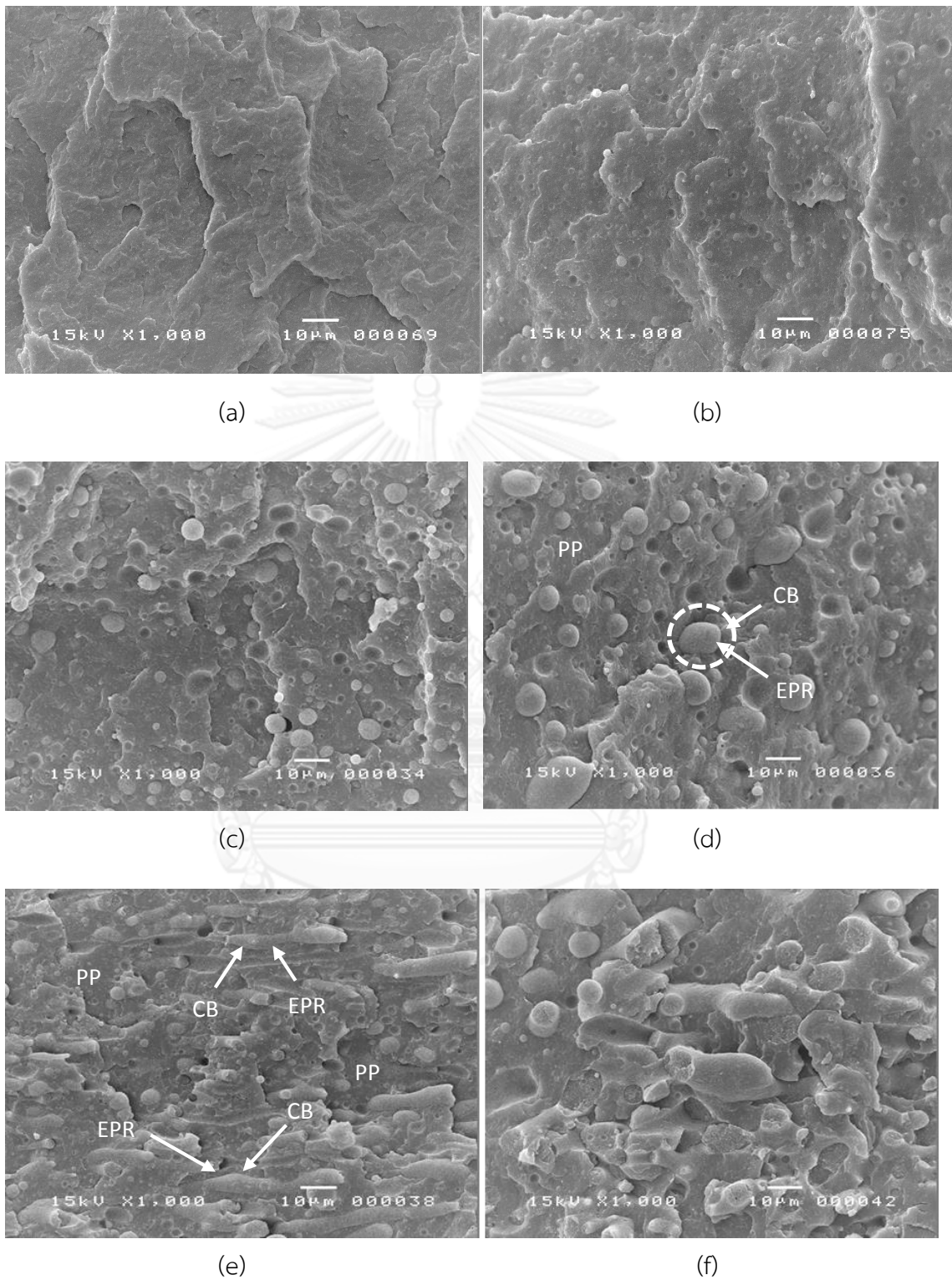
Figure 5. 12: SEM micrographs of freeze-fracture surface of 5 wt% CB-filled PP/EPR blends at various blend ratios: (a) 100/0 (b) 90/10 (c) 80/20 (d) 70/30 (e) 60/40 and (f) 50/50.
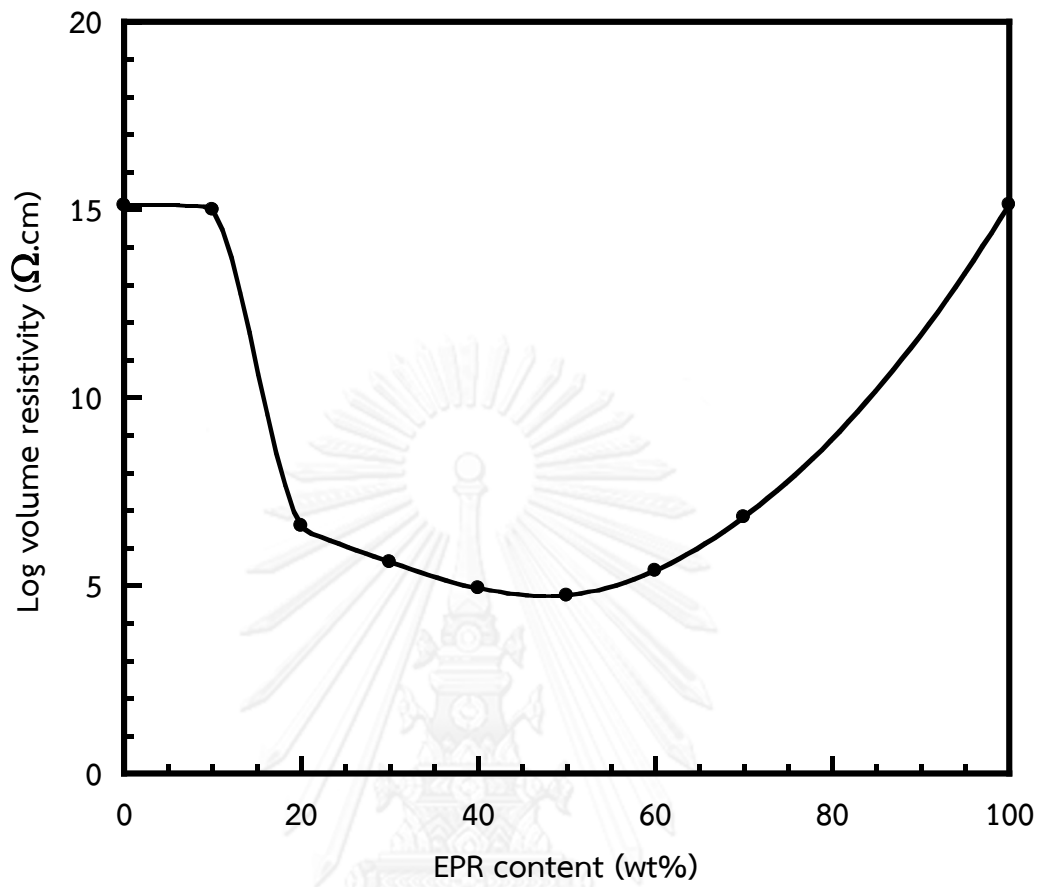
Table 5. 5: Volume resistivity of PP/EPR/CB blends with different processing sequences.

Sample composition	Processing sequence	Volume resistivity (Ω.cm)
70/30 PP/EPR 5 wt% CB	Simultaneously melt-blended	4.3×10^5
	(PP + CB)/EPR	1.6×10^6
	(PP + EPR)/CB	5.7×10^5
	(EPR + CB)/PP	4.2×10^5
70/30 PP/EPR 10 wt% CB	Simultaneously melt-blended	2.4×10^3
	(PP + CB)/EPR	8.4×10^3
	(PP + EPR)/CB	2.3×10^3
	(EPR + CB)/PP	2.1×10^3

Figure 5. 13: Tensile modulus of CB-filled PP and PP/EPR blends at various blend ratios: (●) 100/0, (■) 90/10, (◆) 80/20, (▲) 70/30, (□) 60/40 and (△) 50/50.
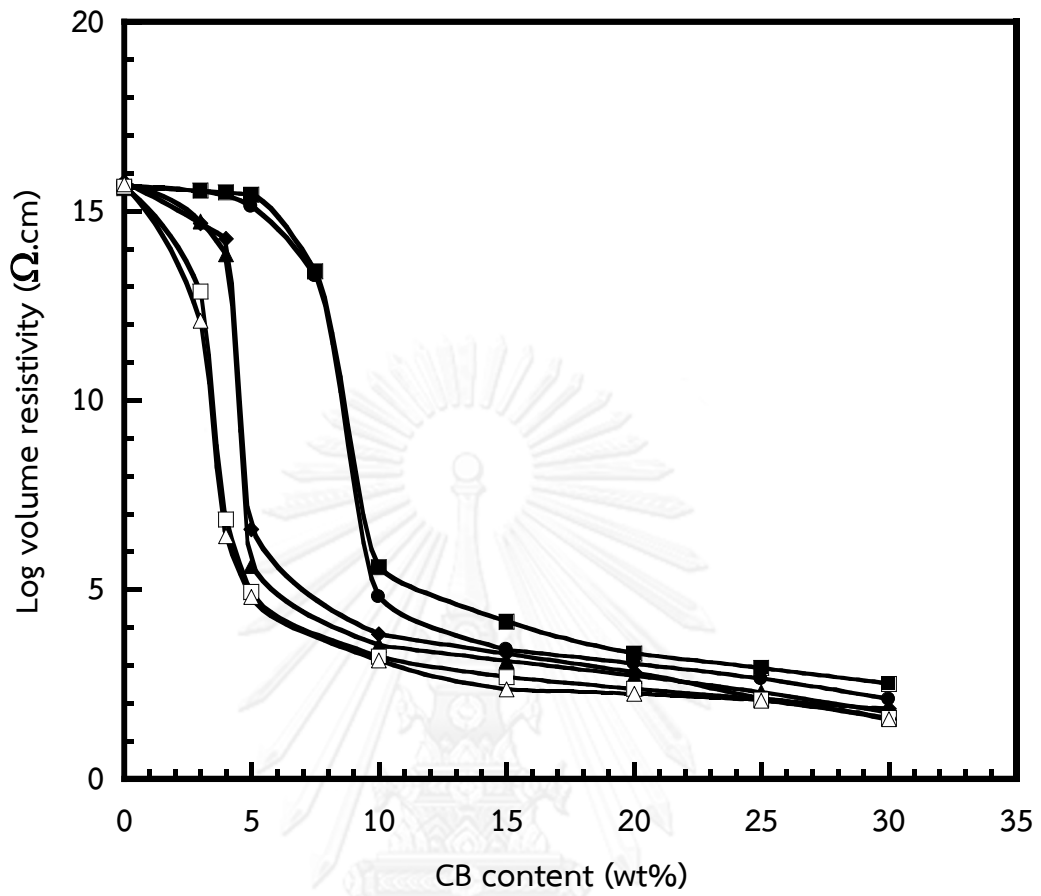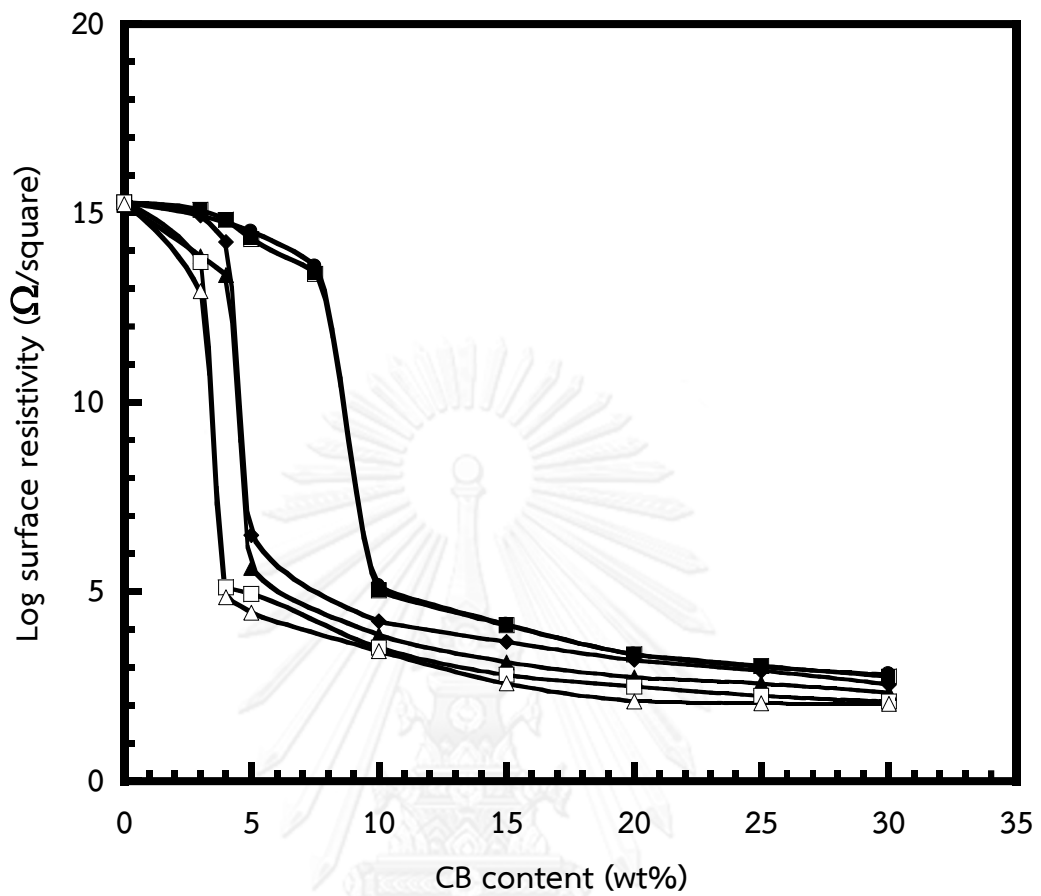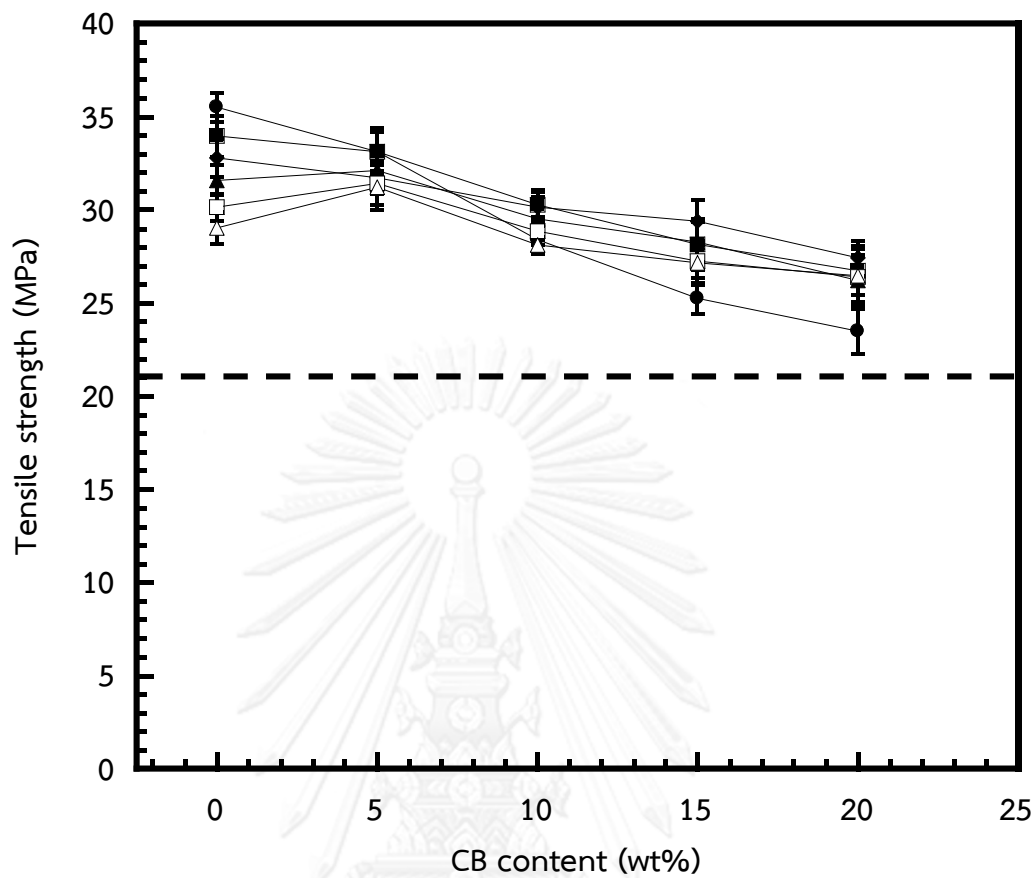
Figure 5. 14: Tensile strength of CB-filled PP and PP/EPR blends at various blend ratios: (●) 100/0, (■) 90/10, (◆) 80/20, (▲) 70/30, (□) 60/40 and (△) 50/50.

Note: (---) Target values of commercial conductive PP are higher than 21 MPa.

Figure 5. 15: Elongation at break of CB-filled PP and PP/EPR blends at various blend ratios: (●) 100/0, (■) 90/10, (◆) 80/20, (▲) 70/30, (□) 60/40 and (△) 50/50.
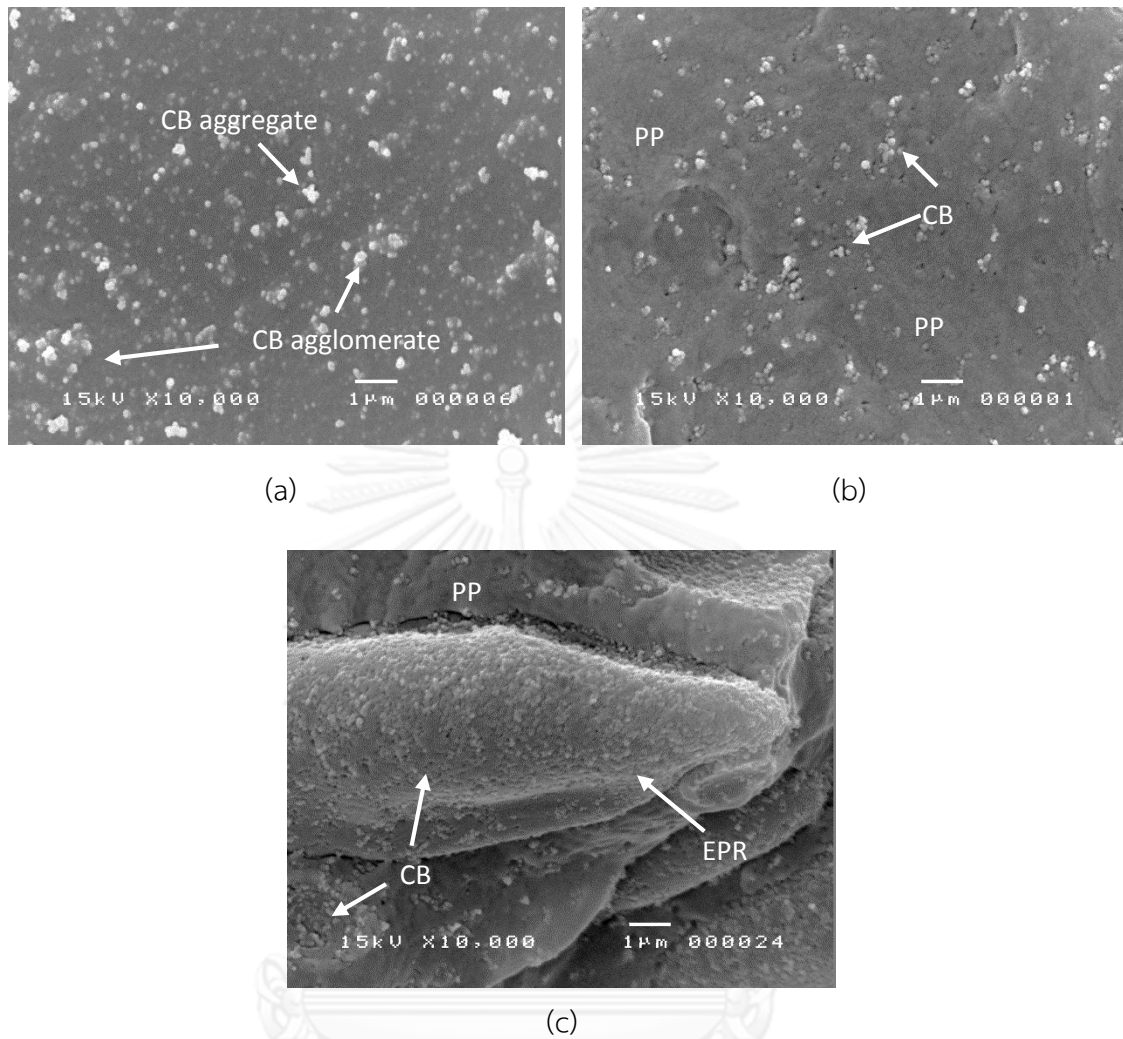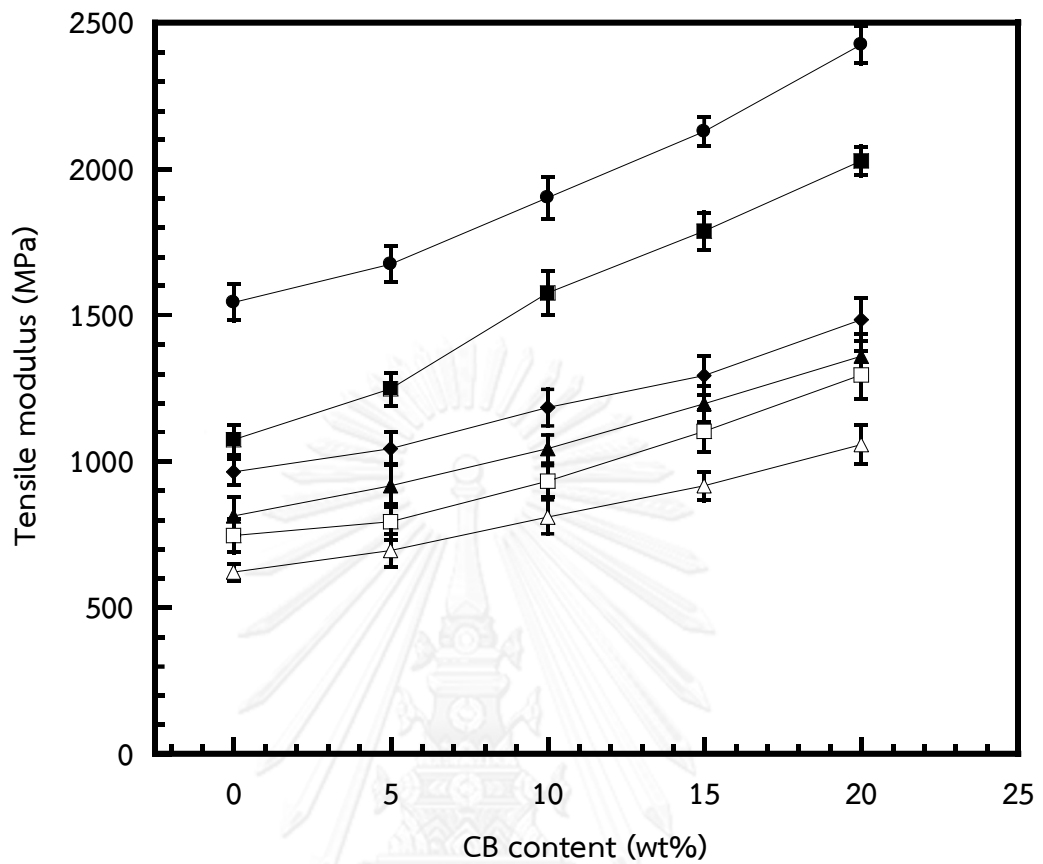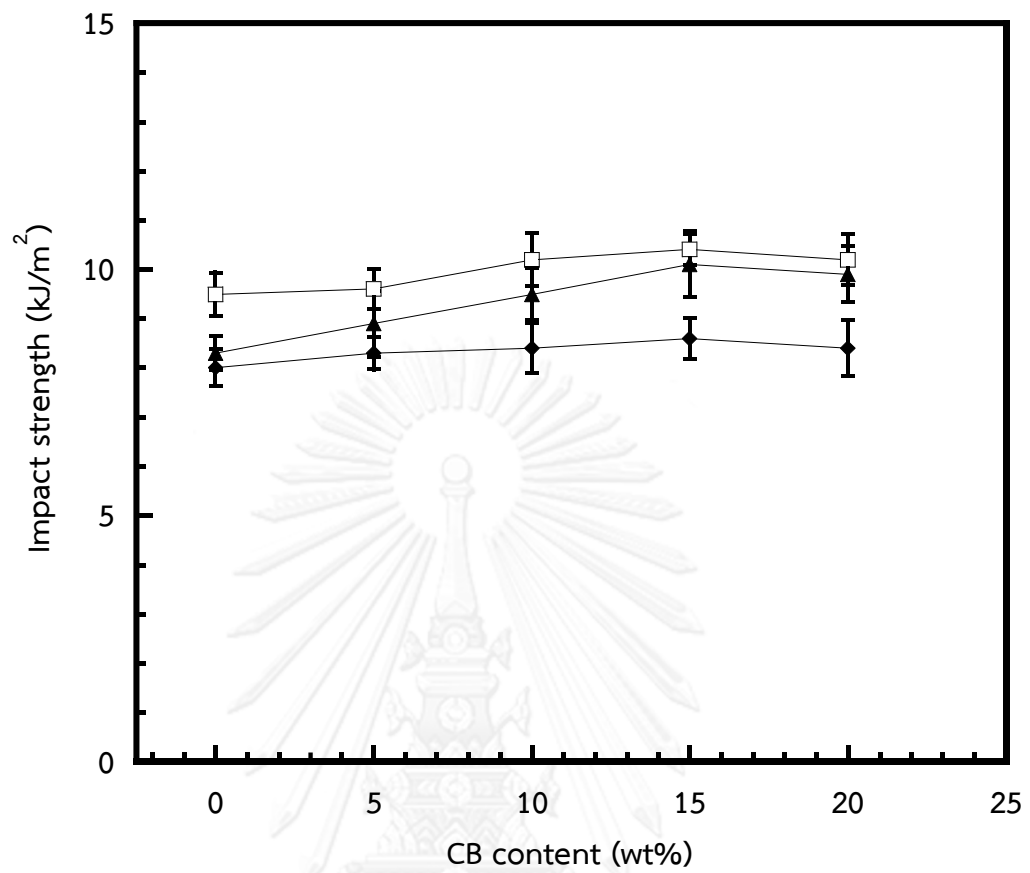
Figure 5. 16: Impact strength of CB-filled PP/EPR blends at various blend ratios: (◆) 80/20, (▲) 70/30 and (□) 60/40.
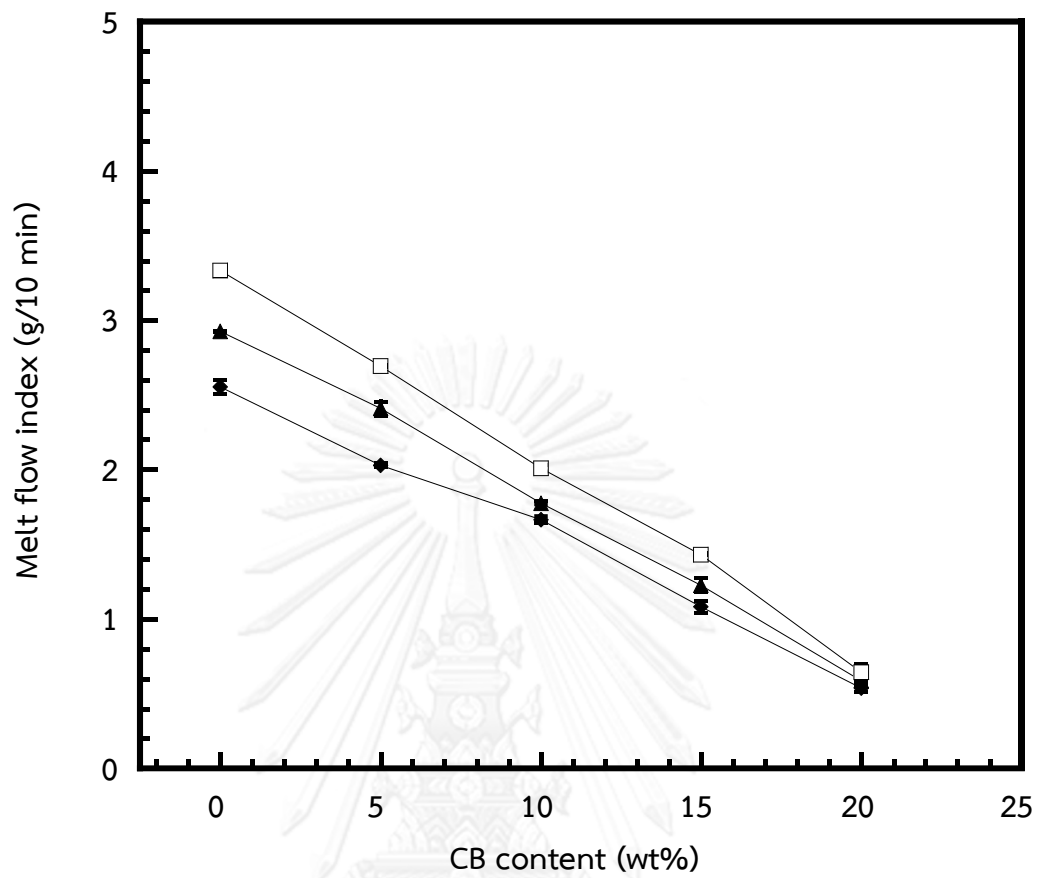
Figure 5. 17: Melt flow index of CB-filled PP/EPR blends at various blend ratios: (◆) 80/20, (▲) 70/30 and (☐) 60/40.

Table 5. 6: Melt flow index of CB-filled PP/EPR blends at various blend ratio.

(Test condition: temperature = 230°C, applied load = 2.16 kg, preheating time = 3 min)

PP/EPR blend ratio	MFI (g/10min)				
	0 wt% CB	5 wt% CB	10 wt% CB	15 wt% CB	20 wt% CB
80:20	2.5±0.05	2.0±.0.05	1.7±0.03	1.1±.0.04	0.5±0.02
70:30	2.9±.01	2.4±0.05	1.8±0.01	1.2±0.05	0.6±0.01
60:40	3.3±.03	2.7±0.01	2.0±0.02	1.4±0.01	0.7±0.05
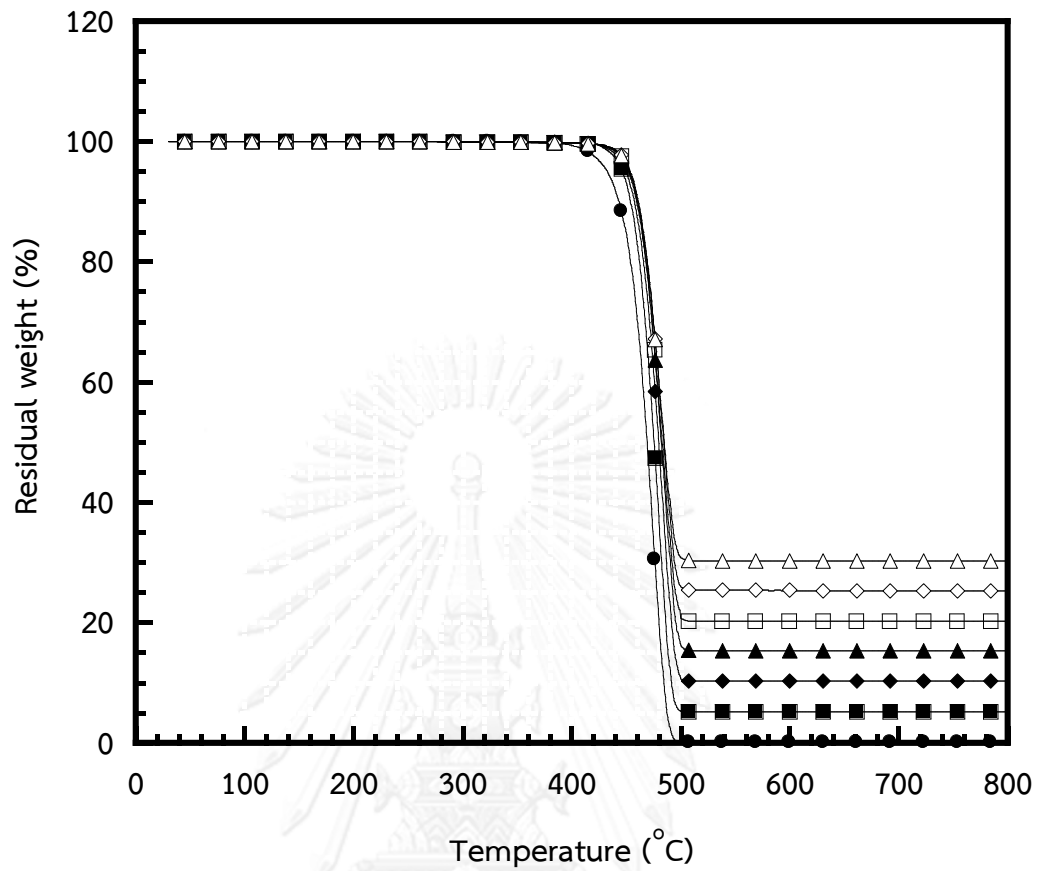
Figure 5. 18: Thermogravimetric analysis (TGA) of CB-filled PP/EPR blend ratio (70/30) at various CB contents: (●) 0 wt%, (■) 5 wt%, (◆) 10 wt%, (▲) 15 wt%, (□) 20 wt%, (◇) 25 wt%, and (△) 30 wt%.
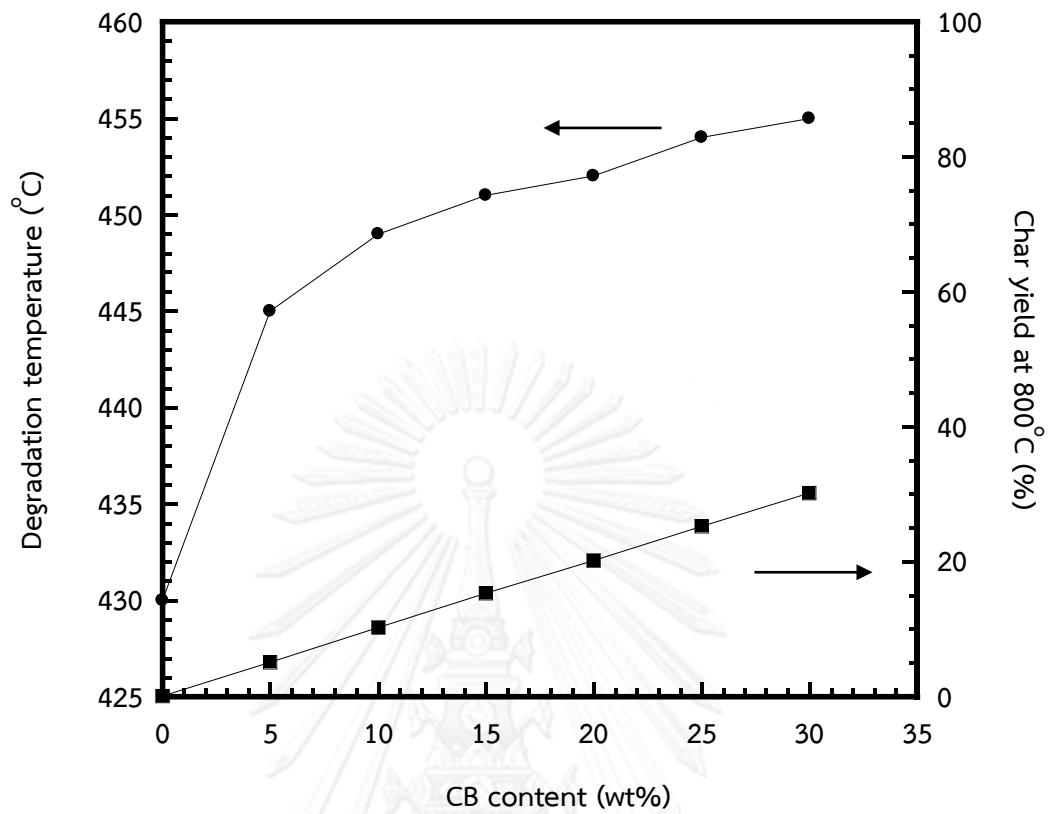
Figure 5. 19: (●) Degradation temperature (5% weight loss) of CB-filled PP/EPR blend ratio of 70/30 and (■) char yield at 800ºC.

Table 5. 7: Degradation temperature and residual char of CB-filled PP/EPR blend ratio of 70/30 at various CB contents.

CB content (wt%)	Degradation temperature (^{o}C) at 5% weight loss	Char yield (%) at 800°C
0	430	0.1
5	445	5.1
10	449	10.3
15	451	15.3
20	452	20.2
25	454	25.3
30	455	30.2
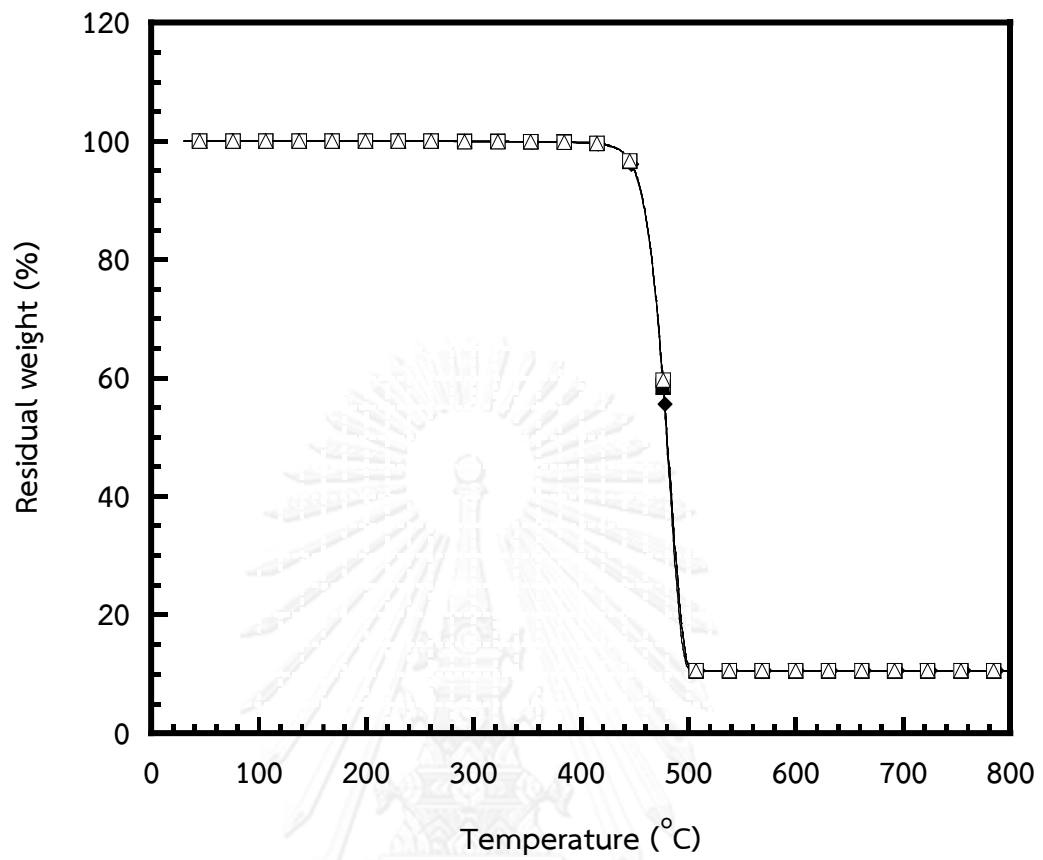
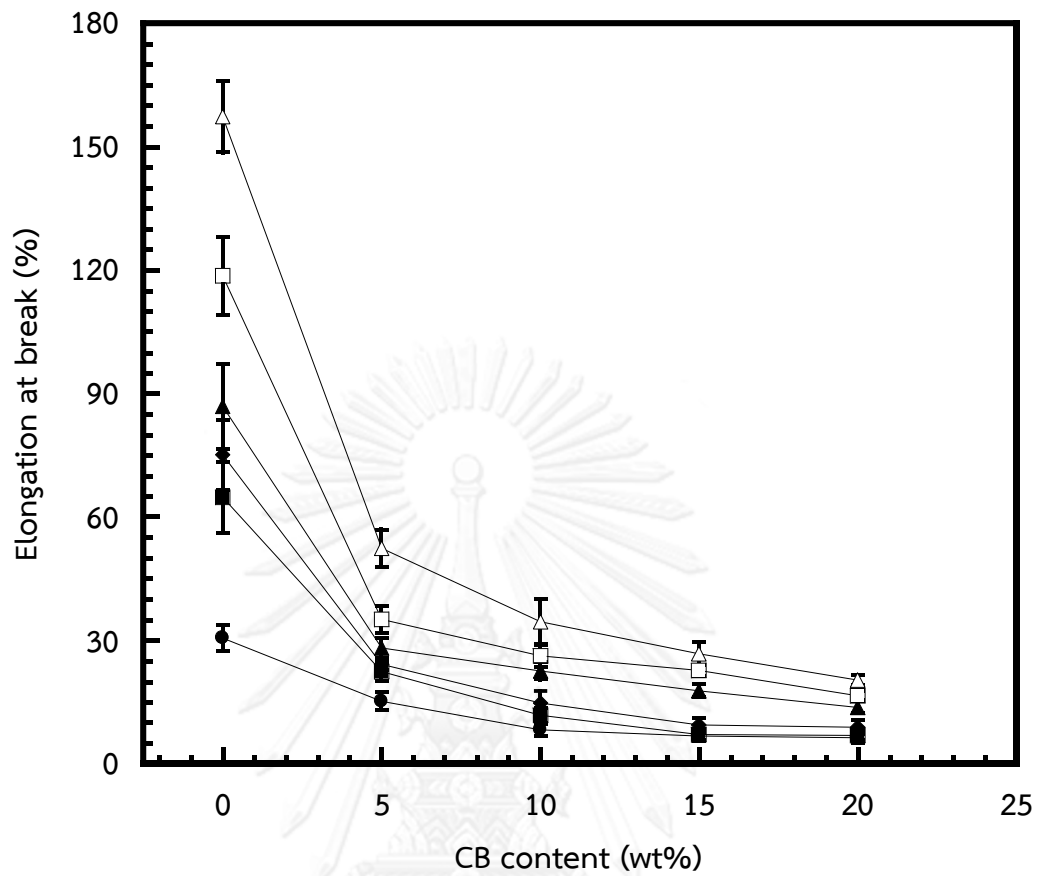**Figure 5. 20:** Thermogravimetric analysis (TGA) of 10 wt% of CB-filled PP/EPR blends at various blend ratios: (●) 100/0, (■) 90/10, (◆) 80/20, (▲) 70/30, (□) 60/40 and (△) 50/50.

**Table 5. 8:** Degradation temperature and residual char of 10 wt% CB-filled PP/EPR blend at various blend ratios.

PP/EPR blend ratio	Degradation temperature (°C) at 5% weight loss	Char yield (%) at 800°C
100/0	450	10.1
90/10	449	10.2
80/20	449	10.2
70/30	449	10.3
60/40	450	10.1
50/50	449	10.2

CHAPTER VI

CONCLUSION

1. PP/EPR blends exhibited two glass transition temperature (T_gs). Both T_gs of PP and EPR phases shifted towards each other suggesting the partially miscible nature of the PP/EPR blends.

2. CB loading in conductive polypropylene compound can be minimized through a double percolation approach.

3. PP/EPR blends exhibited lower percolation thresholds and greater conductivities than those of the CB-filled PP.

4. Percolation threshold of PP/EPR/CB composite with PP/EPR ratio of 60/40 and 50/50 was only about 3 wt% CB.

5. Tensile modulus values of all PP/EPR/CB composites increased with increasing CB content whereas the modulus of PP/EPR/CB composites decreased with increasing EPR content.

6. Tensile strength values for all PP/EPR/CB composites decreased slightly with increasing CB content. The strength values, however, remain higher than that of the commercial one.

7. Melt flow index of all PP/EPR/CB composites increased steadily with increasing of EPR content. Nevertheless, the melt flow index for PP/EPR/CB composites was decreased with increasing CB content.

8. Both degradation temperature (Td) and char yield of all PP/EPR/CB composites were observed to increase with an increase of CB content.

9. The recommended conductive PP compound should be 10 wt% CB-filled PP/EPR blend ratio of 70/30.

REFERENCES

[1] Carbot corporation, *Electrostatic Discharge*. 2013 25.5.2013].

[2] Narkis, M., Lidor, G., Vaxman, A., and Zuri, L., Novel electrically conductive injectionmoldable thermoplastic composites for ESD applications, in Conductive polymers and plastics in industrial applications, L. Rupprecht, Editor. 1999, Plastic Design Library: Norwich. p. 209–217.

[3] EDS Association, *Fundamentals of electrostatic discharge – part 1 an introduction to ESD*. 2013 1.6.2013].

[4] Al-Saleh, M.H. and Sundararaj, U., A review of vapor grown carbon nanofiber/polymer conductive composites. Carbon, 2009. 47(1): p. 2-22.

[5] Tang, H., Chen, X.F., Tang, A.Q., and Luo, Y.X., Studies on the electrical conductivity of carbon black filled polymers. Journal of Applied Polymer Science, 1996. 59(3): p. 383-387.

[6] Gkourmpis, T., Svanberg, C., Kaliappan, S.K., Schaffer, W., Obadal, M., Kandioller, G., and Tranchida, D., Improved electrical and flow properties of conductive polyolefin blends: Modification of poly(ethylene vinyl acetate) copolymer/carbon black with ethylene-propylene copolymer. European Polymer Journal, 2013. 49(8): p. 1975-1983.

[7] Levon, K., Margolina, A., and Patashinsky, A.Z., Multiple percolation in   conducting polymer blends. Macromolecules, 1993. 26(15): p. 4061-4063.

[8] Mallette, J.G., Quej, L.M., Marquez, A., and Manero, O., Carbon black-filled PET/HDPE blends: Effect of the CB structure on rheological and electric properties. Journal of Applied Polymer Science, 2001. 81(3): p. 562-569.

[9] Wu, G.Z., Li, B.P., and Jiang, J.D., Carbon black self-networking induced co-continuity of immiscible polymer blends. Polymer, 2010. 51(9): p. 2077-2083.

[10] Al-Saleh, M.H. and Sundararaj, U., Nanostructured carbon black filled polypropylene/polystyrene blends containing styrene-butadiene-styrene copolymer: Influence of morphology on electrical resistivity. European Polymer Journal, 2008. 44(7): p. 1931-1939.

[11] Farshidfar, A., Haddadi, V., and Nazokdast, H. Electrical and mechanical properties of conductive carbon black/polyolefin composites mixed with carbon fiber. in Convention and Trade Show American Composite Manufactures Association. 2006. St. Louis, MO, USA: Composites.

[12] Dai, K., Xu, X.B., and Li, Z.M., Electrically conductive carbon black (CB) filled in situ microfibrillar poly(ethylene terephthalate) (PET)/polyethylene (PE) composite

with a selective CB distribution. <u>Polymer</u>, 2007. 48(3): p. 849-859.

[13] Shen, L., Wang, F.Q., Yang, H., and Meng, Q.R., The combined effects of carbon black and carbon fiber on the electrical properties of composites based on polyethylene or polyethylene/polypropylene blend. <u>Polymer Testing</u>, 2011. 30(4): p. 442-448.

[14] Mekhilef, N. and Verhoogt, H., Phase inversion and dual-phase continuity in polymer blends: Theoretical predictions and experimental results. <u>Polymer</u>, 1996. 37(18): p. 4069-4077.

[15] Skochdopole, R.E., Finch, C.R., and Marshall, J., Properties and morphology of some injection-molded polycarbonate/styrene-acrylonitrile copolymer blend. <u>Polymer Engineering & Science</u>, 1987. 27: p. 627-631.

[16] Heeschen, W.A., A Quantitative image-analysis method for the determination of cocontinuity in polymer blends. <u>Polymer</u>, 1995. 36(9): p. 1835-1841.

[17] Avgeropoulos, G.N., Wessert, F.C., and Boehm, G.A., Heterogeneous blends of polymers: Rheology and morphology. <u>Rubber Chemistry and Technology</u>, 1976. 40: p. 93-104.

[18] Paul, D.R. and Barlow, J.W., Polymer Blends. <u>Journal of Macromolecular Science: Part C: Polymer Reviews</u>, 1980. 18: p. 109-168.

[19] Accorsi, J.V., *The impact of carbon black morphology and dispersion on the weatherability of polyethylene*, in *Paper presented at the International Wire & Cable Symposium*1999: Atlantic City.

[20] Huang, J.C., Carbon black filled conducting polymers and polymer blends. <u>Advances in Polymer Technology</u>, 2002. 21(4): p. 299-313.

[21] Leblanc, J.L., <u>Filled polymers: Science and industrial applications</u>. 2010, USA: Taylor & Francis Group.

[22] Al-Saleh, M.H. and Sundararaj, U., An innovative method to reduce percolation threshold of carbon black filled immiscible polymer blends. <u>Composites Part a-Applied Science and Manufacturing</u>, 2008. 39(2): p. 284-293.

[23] Hussain, M., Choa, Y.H., and Niihara, K., Fabrication process and electrical behavior of novel pressure-sensitive composites. <u>Composites Part a-Applied Science and Manufacturing</u>, 2001. 32(12): p. 1689-1696.

[24] Badesha, S.S. and Swift, J.A., Practical surfaces: beyond the wheel. <u>Surface Science</u>, 2002. 500(1-3): p. 1024-1041.

[25] Mamunya, Y., Polymer blends filled with carbon black: Structure and electrical properties. <u>Macromolecular Symposia</u>, 2001. 170: p. 257-264.

[26] Mamunya, Y.P., Muzychenko, Y.V., Pissis, P., Lebedev, E.V., and Shut, M.I.,

Percolation phenomena in polymers containing dispersed iron. <u>Polymer Engineering and Science</u>, 2002. 42(1): p. 90-100.

[27] Feng, J.Y., Chan, C.M., and Li, J.X., A method to control the dispersion of carbon black in an immiscible polymer blend. <u>Polymer Engineering and Science</u>, 2003. 43(5): p. 1058-1063.

[28] Fenouillot, F., Cassagnau, P., and Majeste, J.C., Uneven distribution of nanoparticles in immiscible fluids: Morphology development in polymer blends. <u>Polymer</u>, 2009. 50(6): p. 1333-1350.

[29] Wu, S., Interfacial and surface tensions of polymers. <u>Journal of Macromolecular Science: Part C: Polymer Reviews</u>, 1974. 10: p. 1-73.

[30] Cheah, K., Forsyth, M., and Simon, G.P., Processing and morphological development of carbon black filled conducting blends using a binary host of poly(styrene co-acrylonitrile) and poly(styrene). <u>Journal of Polymer Science Part B-Polymer Physics</u>, 2000. 38(23): p. 3106-3119.

[31] Cui, L.M., Zhang, Y., Zhang, Y.X., Zhang, X.F., and Zhou, W., Electrical properties and conductive mechanisms of immiscible polypropylene/Novolac blends filled with carbon black. <u>European Polymer Journal</u>, 2007. 43(12): p. 5097-5106.

[32] Foulger, S.H., Reduced percolation thresholds of immiscible conductive blends. <u>Journal of Polymer Science Part B-Polymer Physics</u>, 1999. 37(15): p. 1899-1910.

[33] Chan, C.M., Cheng, C.L., and Yuen, M.M.F., Electrical properties of polymer composites prepared by sintering a mixture of carbon black and ultra-high molecular weight polyethylene powder. <u>Polymer Engineering and Science</u>, 1997. 37(7): p. 1127-1136.

[34] Sumita, M., Sakata, K., Hayakawa, Y., Asai, S., Miyasaka, K., and Tanemura, M., Double percolation effect on the electrical conductivity of conductive particles filled polymer blends. <u>Colloid & Polymer Science</u>, 1992. 270: p. 134-139.

[35] Di, W.H., Zhang, G., Peng, Y., and Zhao, Z.D., Two-step PTC effect in immiscible polymer blends filled with carbon black. <u>Journal of Materials Science</u>, 2004. 39(2): p. 695-697.

[36] Thielen, A., Valange, B., and Viering, S., Conductive polymer blends with finely divided conductive material selectively localized in continuous polymer phase or continuous interface, in United States Patent2001, Cabot Corporation, Boston, MA: USA.

[37] Naiki, M., Matsumura, T., and Matsuda, M., Tensile elongation of high-fluid polypropylene/ethylene-propylene rubber blends: Dependence on molecular weight of the components and propylene content of the rubber. Journal of Applied Polymer Science, 2002. 83(1): p. 46-56.

[38] Qin, J.L., Guo, S.Q., and Li, Z.T., Melting behavior and isothermal crystallization kinetics of PP/mLLDPE blends. Journal of Polymer Research, 2008. 15(5): p. 413-420.

[39] Xu, S.X., Wen, M., Li, J., Guo, S.Y., Wang, M., Du, Q., Shen, J.B., Zhang, Y.Q., and Jiang, S.L., Structure and properties of electrically conducting composites consisting of alternating layers of pure polypropylene and polypropylene with a carbon black filler. Polymer, 2008. 49(22): p. 4861-4870.

[40] Dang, Z.M., Yuan, J.K., Zha, J.W., Zhou, T., Li, S.T., and Hu, G.H., Fundamentals, processes and applications of high-permittivity polymer matrix composites. Progress in Materials Science, 2012. 57(4): p. 660-723.

[41] Nitta, K., Kawada, T., Yamahiro, M., Mori, H., and Terano, M., Polypropylene-block-poly(ethylene-co-propylene) addition to polypropylene/poly (ethylene-co-propylene) blends: morphology and mechanical properties. Polymer, 2000. 41(18): p. 6765-6771.

[42] Li, R.B., Zhang, X.Q., Zhao, Y., Hu, X.T., Zhao, X.T., and Wang, D.J., New polypropylene blends toughened by polypropylene/poly(ethylene-co-propylene) in-reactor alloy: Compositional and morphological influence on mechanical properties. Polymer, 2009. 50(21): p. 5124-5133.

[43] Morton-Jones, D.H., Polymer processing. 1993: London : Chapman & Hall.

[44] Gubbels, F., Blacher, S., Vanlathem, E., Jerome, R., Deltour, R., Brouers, F., and Teyssie, P., Design of electrical conductive composites - Key role of the morphology on the electrical-properties of carbon-black filled polymer blends. Macromolecules, 1995. 28(5): p. 1559-1566.

[45] Pour, S.A.H., Pourabbas, B., and Hosseini, M.S., Electrical and rheological properties of PMMA/LDPE blends filled with carbon black. Materials Chemistry and Physics, 2014. 143(2): p. 830-837.

[46] Xu, Z.B., Zhao, C., Gu, A.J., and Fang, Z.P., Electric conductivity of PS/PA6/carbon black composites. Journal of Applied Polymer Science, 2007. 103(2): p. 1042-1047.

[47] Naficy, S. and Garmabi, H., Study of the effective parameters on mechanical and electrical properties of carbon black filled PP/PA6 microfibrillar composites. Composites Science and Technology, 2007. 67(15-16): p. 3233-3241.

[48] Zoldan, J., Siegmann, A., and Narkis, M., Polypropylene/nylon-66/carbon black blends processed at temperatures just below the nylon melting: Anisotropy in structure and properties. Macromolecular Symposia, 2006. 233: p. 123-131.

[49] Brigandi, P.J., Cogen, J.M., and Pearson, R.A., Electrically conductive multiphase polymer blend carbon-based composites. Polymer Engineering and Science, 2014. 54(1): p. 1-16.

[50] Bruna, J., Yazdani-Pedram, M., Quijada, R., Valentin, J.L., and Lopez-Manchado, M.A., Melt grafting of itaconic acid and its derivatives onto an ethylene-propylene copolymer. Reactive & Functional Polymers, 2005. 64(3): p. 169-178.

[51] Breuer, O., Tchoudakov, R., Narkis, M., and Siegmann, A., Segregated structures in carbon black-containing immiscible polymer blends: HIPS/LLDPE systems. Journal of Applied Polymer Science, 1997. 64(6): p. 1097-1106.

[52] De, D., Panda, P.K., Roy, M., and Bhunia, S., Reinforcing effect of reclaim rubber on natural rubber/polybutadiene rubber blends. Materials & Design, 2013. 46: p. 142-150.

[53] Kaynak, A., Polat, A., and Yilmazer, U., Some microwave and mechanical properties of carbon fiber-polypropylene and carbon black-polypropylene composites. Materials Research Bulletin, 1996. 31(10): p. 1195-1206.

[54] Huang, J.C. and Wu, C.L., Processability, mechanical properties, and electrical conductivities of carbon black-filled ethylene-vinyl acetate copolymers. Advances in Polymer Technology, 2000. 19(2): p. 132-139.

[55] Carbot corporation, Raw materials catalog. 2013 1.6.2013].

[56] Asuke, F., Aigbodion, V.S., Abdulwahab, M., Fayomi, O.S.I., Popoola, A.P.I., Nwoyi, C.I., and Garba, B., Effects of bone particle on the properties and microstructure of polypropylene/bone ash particulate composites. Results in Physics, 2012. 2: p. 135-141.

[57] Lee, S.H., Kontopoulou, M., and Park, C.B., Effect of nanosilica on the co-continuous morphology of polypropylene/polyolefin elastomer blends. Polymer, 2010. 51(5): p. 1147-1155.

[58] Kashiwagi, T., Grulke, E., Hilding, J., Harris, R., Awad, W., and Douglas, J., Thermal degradation and flammability properties of poly(propylene)/carbon nanotube composites. Macromolecular Rapid Communications, 2002. 23(13): p. 761-765.

[59] Wen, X., Wang, Y.J., Gong, J., Liu, J., Tian, N.N., Wang, Y.H., Jiang, Z.W., Qiu, J., and Tang, T., Thermal and flammability properties of polypropylene/carbon black nanocomposites. Polymer Degradation and Stability, 2012. 97(5): p. 793-801.

[60] Zhang, Y.D., Xiang, J.J., Zhang, Q., Liu, Q.F., and Frost, R.L., Influence of kaolinite/carbon black hybridization on combustion and thermal decomposition behaviors of NR composites. Thermochimica Acta, 2014. 576: p. 39-46.

APPENDIX

Requirement for Conductive Polypropylene Packaging

Property	Condition	Unit	Value
Density	$23\pm2^{o}C$	g/cm^{3}	1.09-1.208
Melt flow rate	$230^{o}C/2.16$ kg	$g/10$ min	0.4-4.6
	$230^{o}C/5$ kg		2.3-20.5
	$230^{o}C/10$ kg		10.3-94
Tensile strength at break	50 mm/min	MPa	15-19.5
Tensile strength at yield	50 mm/min	MPa	21-27.5
Elongation at break	50 mm/min	%	20-59
Flexural modulus	-	MPa	942-1500
Notched izod impact	$23\pm2^{o}C$	kJ/m^{2}	9.3-45
Volume resistivity	$23\pm2^{o}C$	$\Omega \cdot cm$	$20\text{-}10^{4}$
Surface resistivity	$23\pm2^{o}C$	Ω/sq	$2\times10^{2}\text{-}10^{6}$

VITA

Mr. Sarote Phromdee was born in Ratchaburi, Thailand. He graduated at high school level in 2006 from Benchamarachuthit Chanthaburi School. He received the Bachelor's Degree of Engineering with a major in Chemical Engineering from the Faculty of Engineer, Mahanakorn University of Technology, Thailand in 2011. After graduation, he furthers his study for a Master's Degree of Chemical Engineering at the Department of Chemical Engineering, Faculty of Engineering, Chulalongkorn University.

Some parts of this work were selected for poster presentations in 1) The Eighth Pure and Applied Chemistry International Conference (PACCON) on Moving Towards Innovation in Chemistry which was held during January 8-10, 2014 at Centara Hotel and Convention Centre, Khon Kaen, Thailand and 2) Asian Polymer Association (APA) International Conference on Polymers: Vision & Innovation which was held during February 19-21, 2014 at India Habitat Centre, New Delhi, India